

**Academic Year 2016-2017**

Faculty Pharmaceutical, Biomedical and Veterinary Sciences

Biochemistry and Biotechnology

## IONIZING RADIATION: A ROAD TO A SENESCENT CARDIOVASCULAR SYSTEM?

By:

**Liese De Ridder**

*Master Thesis in partial fulfillment of the requirements for the degree*

***Master in Biochemistry and Biotechnology***

Promotor University of Antwerp: Prof. Dr. Sylvia Dewilde

Copromotor SCK•CEN: Dr. Ir. An Aerts

Coaches: Dr. Ir. An Aerts and Bjorn Baselet (PhD student)

Belgian Nuclear Research Centre (SCK•CEN)

Radiobiology unit

Boeretang 200

2400 Mol









# TABLE OF CONTENTS

---

<b>TABLE OF CONTENTS</b> .....	<b>I</b>
<b>LIST OF FIGURES</b> .....	<b>III</b>
<b>LIST OF ABBREVIATIONS</b> .....	<b>V</b>
<b>ACKNOWLEDGEMENTS</b> .....	<b>VII</b>
<b>SAMENVATTING</b> .....	<b>IX</b>
<b>ABSTRACT</b> .....	<b>XI</b>
<b>1 INTRODUCTION</b> .....	<b>1</b>
1.1 IONIZING RADIATION: A RISK FACTOR FOR CARDIOVASCULAR DISEASE .....	1
1.1.1 <i>Ionizing radiation</i> .....	1
1.1.2 <i>Epidemiological evidence</i> .....	3
1.2 RADIATION-INDUCED CARDIOVASCULAR DISEASE .....	5
1.2.1 <i>Atherosclerosis is the main cause of cardiovascular disease</i> .....	5
1.2.2 <i>Pro-atherosclerotic effects of ionizing radiation</i> .....	6
1.3 RELEVANCE OF ENDOTHELIAL SENESENCE IN CARDIOVASCULAR DISEASE .....	7
1.3.1 <i>Mechanisms of cellular senescence</i> .....	7
1.3.2 <i>Senescent endothelial cells play a role in cardiovascular disease</i> .....	8
1.3.3 <i>Biomarker for the identification of senescent cells</i> .....	9
1.4 CANDIDATE MODULATORS OF PREMATURE SENESENCE .....	9
1.4.1 <i>IGF-1</i> .....	9
1.4.2 <i>Statins</i> .....	11
1.4.3 <i>Ascorbic acid</i> .....	12
1.4.4 <i>Hydrocortisone</i> .....	13
1.4.5 <i>Rosiglitazone</i> .....	13
1.5 RESEARCH AIMS AND OBJECTIVES .....	14
<b>2 MATERIALS AND METHODS</b> .....	<b>15</b>
2.1 CELL CULTURE .....	15
2.2 IRRADIATION .....	15
2.3 STANDARD SENESENCE-ASSOCIATED B-GALACTOSIDASE ASSAY .....	15
2.4 CPRG ASSAY .....	15
2.5 MUG ASSAY .....	16
2.6 ATORVASTATIN CYTOTOXICITY TEST USING MTT CELL VIABILITY ASSAY .....	16
2.7 PROTEIN EXTRACTION AND WESTERN BLOT .....	16
2.8 NITRIC OXIDE ASSAY .....	17
2.9 IMMUNOCYTOCHEMICAL STAINING .....	17
2.10 STATISTICS .....	17
<b>3 RESULTS</b> .....	<b>19</b>
3.1 DETECTION OF RADIATION-INDUCED SENESENCE USING THREE DIFFERENT ASSAYS .....	19
3.2 EFFECT OF ATORVASTATIN ON ENDOTHELIAL CELL VIABILITY .....	20
3.3 EFFECT OF DIFFERENT COMPOUNDS ON RADIATION-INDUCED SENESENCE IN ENDOTHELIAL CELLS .....	20
3.4 EFFECT OF HYDROCORTISONE ON RADIATION-INDUCED EXPRESSION OF P21 AND P16 .....	21
3.5 EFFECT OF RADIATION AND HYDROCORTISONE TREATMENT ON NITRIC OXIDE PRODUCTION BY ENDOTHELIAL CELLS .....	22
3.6 IMMUNOCYTOCHEMICAL STAINING OF ENDOTHELIAL CELLS .....	23
<b>4 DISCUSSION</b> .....	<b>27</b>
4.1 IONIZING RADIATION INDUCES SENESENCE IN HUMAN CORONARY ARTERY ENDOTHELIAL CELLS .....	27

4.2	ATORVASTATIN INDUCES CELL DEATH IN HUMAN CORONARY ARTERY ENDOTHELIAL CELLS.....	27
4.3	EFFECT OF DIFFERENT COMPOUNDS ON RADIATION-INDUCED SENESCENCE IN ENDOTHELIAL CELLS .....	28
4.4	HYDROCORTISONE TREATMENT REDUCES P21 EXPRESSION IN HUMAN CORONARY ARTERY ENDOTHELIAL CELLS .....	30
4.5	HYDROCORTISONE TREATMENT REDUCES NITRIC OXIDE PRODUCTION BY HUMAN CORONARY ARTERY ENDOTHELIAL CELLS.....	32
4.6	IRRADIATION INCREASES CELL SIZE, SENESCENCE-ASSOCIATED $\beta$ -GALACTOSIDASE ACTIVITY AND P21 EXPRESSION IN ENDOTHELIAL CELLS .....	32
<b>5</b>	<b>CONCLUSION .....</b>	<b>35</b>
<b>7</b>	<b>REFERENCES.....</b>	<b>37</b>
<b>8</b>	<b>SUPPLEMENTARY INFORMATION .....</b>	<b>45</b>

## LIST OF FIGURES

---

<b>Figure 1:</b> Direct and indirect mechanisms of radiation-induced DNA damage .....	2
<b>Figure 2:</b> Increase in risk of cardiovascular diseases after exposure to ionizing radiation.....	3
<b>Figure 3:</b> Stages in the development of atherosclerotic lesions.....	6
<b>Figure 4:</b> Pathways involved in the induction of senescence .....	7
<b>Figure 5:</b> Phenotypic changes in senescent endothelial cells and their pathophysiological consequences .....	9
<b>Figure 6:</b> Summary of the effects induced by insulin-like growth factor-1 signaling. ....	10
<b>Figure 7:</b> Summary of the effects induced by atorvastatin.....	12
<b>Figure 8:</b> Senescence-associated $\beta$ -galactosidase activity (SA $\beta$ -gal) in irradiated HCAECs. ....	19
<b>Figure 9:</b> Effect of atorvastatin on HCAEC viability after 24 h of treatment.....	20
<b>Figure 10:</b> Senescence-associated $\beta$ -galactosidase (SA $\beta$ -gal) activity in irradiated HCAECs treated with different compounds.....	21
<b>Figure 11:</b> p21 protein expression in irradiated HCAECs treated with hydrocortisone.....	22
<b>Figure 12:</b> Intracellular nitric oxide (NO) bioavailability in irradiated HCAECs treated with hydrocortisone. ....	22
<b>Figure 13:</b> Immunocytochemical stainings of irradiated HCAECs treated with hydrocortisone. ....	23
<b>Figure 14:</b> Ionizing radiation increases cell size, senescence-associated $\beta$ -galactosidase activity and p21 protein levels in HCAECs. ....	24



## LIST OF ABBREVIATIONS

---

<b>4-MU</b>	4-Methylumbelliferone	<b>mTOR</b>	Mammalian target of rapamycin
<b>A.U.</b>	Arbitrary units	<b>MTT</b>	3-(4,5-Didimethylthiazol-2-yl)-2,5-diphenyltetrazolium bromide
<b>ASC</b>	Ascorbic acid	<b>MUG</b>	4-Methylumbelliferyl- $\beta$ -D-galactopyranoside
<b>ATM</b>	Ataxia-telangiectasia mutated	<b>NF<math>\kappa</math>B</b>	Nuclear factor kappa B
<b>ATR</b>	Ataxia-telangiectasia and Rad3-related	<b>NO</b>	Nitric oxide
<b><math>\beta</math>-gal</b>	Beta-galactosidase	<b>OH<math>\cdot</math></b>	Hydroxyl radical
<b>BCA</b>	Bicinchoninic acid	<b>p.i.</b>	Post irradiation
<b>BGG</b>	Bovine gamma globulin	<b>PAI-1</b>	Plasminogen activator inhibitor-1
<b>Bq</b>	Becquerel	<b>PBS</b>	Phosphate buffered saline
<b>BSA</b>	Bovine serum albumin	<b>PECAM</b>	Platelet endothelial cell adhesion molecule
<b>Chk1</b>	Checkpoint kinase 1	<b>PI3K</b>	Phosphatidylinositol 3-kinase
<b>Chk 2</b>	Checkpoint kinase 2	<b>PPAR-<math>\gamma</math></b>	Peroxisome proliferator-activated receptor gamma
<b>CPRG</b>	Chlorophenol red $\beta$ -D-galactopyranoside	<b>pRb</b>	Retinoblastoma protein
<b>CT</b>	Computed tomography	<b>px</b>	Pixel
<b>CTRL</b>	Control	<b>Ras</b>	Rat sarcoma
<b>CVD</b>	Cardiovascular disease	<b>ROS</b>	Reactive oxygen species
<b>DAF-FM</b>	4-Amino-5-methylamino-2',7'-difluorofluorescein	<b>SA <math>\beta</math>-gal</b>	Senescence-associated beta-galactosidase
<b>DAPI</b>	4',6-Diamidino-2-phenylindole	<b>SEM</b>	Standard error of the mean
<b>EC</b>	Endothelial cell	<b>SIRT 1</b>	Sirtuin 1
<b>ECL</b>	Enhanced chemiluminescence	<b>SNOC</b>	S-nitrosocysteine
<b>eNOS</b>	Endothelial nitric oxide synthase	<b>Sv</b>	Sievert
<b>GR</b>	Glucocorticoid receptor	<b>TBS</b>	TRIS-buffered saline
<b>Gy</b>	Gray	<b>TBST</b>	TRIS-buffered saline Triton X-100
<b>HBSS</b>	Hank's Balanced Salt Solution	<b>TGF-<math>\beta</math></b>	Transforming growth factor-beta
<b>HMG-CoA</b>	3-Hydroxy-3-methyl-glutaryl-coenzyme A	<b>TICAE</b>	Telomerase-immortalized coronary artery endothelial cell
<b>HRP</b>	Horseradish peroxidase	<b>TNF-<math>\alpha</math></b>	Tumor necrosis factor-alpha
<b>HUVEC</b>	Human umbilical vein endothelial cell	<b>TZD</b>	Thiazolidinediones
<b>ICAM</b>	Intracellular adhesion molecule	<b>UVA</b>	Ultraviolet A
<b>IFN-<math>\gamma</math></b>	Interferon-gamma	<b>UVB</b>	Ultraviolet B
<b>IGF</b>	Insulin-like growth factor	<b>VCAM</b>	Vascular cell adhesion molecule
<b>IGF1R</b>	IGF-1 receptor	<b>VSMC</b>	Vascular smooth muscle cell
<b>IGFBP</b>	IGF binding protein	<b>W<sub>R</sub></b>	Radiation weighting factor
<b>IL</b>	Interleukin	<b>W<sub>T</sub></b>	Tissue weighting factor
<b>LDL</b>	Low-density lipoprotein	<b>X-gal</b>	5-Bromo-4-chloro-3-indolyl- $\beta$ -D-galactopyranoside
<b>Mdm2</b>	Mouse double minute 2		



## ACKNOWLEDGEMENTS

---

First of all, I would like to express my gratitude towards prof. dr. Sarah Baatout, dr. ir. An Aerts and Bjorn Baselet for giving me the opportunity to fulfill my master thesis at the Radiobiology unit of SCK•CEN. Especially, I would like to thank dr. ir. An Aerts and Bjorn Baselet for guiding me through my internship. Their patience, advice, knowledge and remarks were greatly valued. Moreover, I am particularly grateful to Bjorn Baselet for teaching me all experimental techniques, helping me with data analysis and answering all of my questions. His continuous support, enthusiasm and our chats in the lab were also very much appreciated. Furthermore, I would like to thank prof. dr. Sylvia Dewilde for carefully reading my thesis and providing me with valuable comments. I would also like to express my warm thanks to Niels Belmans for helping me with lab-related, statistical and other questions as well as his unconditional support. Last but not least, I would like to thank the other master students for the great time I had, filled with laughter, gossip and after work events.



## SAMENVATTING

---

Cardiovasculaire aandoeningen zijn de meest voorkomende doodsoorzaak wereldwijd en worden voor een groot deel veroorzaakt door atherosclerose. Cardiovasculaire risicofactoren kunnen opgedeeld worden in twee categorieën, namelijk gedragsgerelateerde risicofactoren zoals roken en gebrek aan lichaamsbeweging en algemene risicofactoren zoals leeftijd en etniciteit. Recente epidemiologische studies hebben aangetoond dat ook blootstelling aan ioniserende straling een risicofactor is voor de ontwikkeling van cardiovasculaire aandoeningen. Endotheelcellen, die de binnenkant van bloedvaten bekleden, worden hierbij beschouwd als een belangrijk doelwit voor ioniserende straling. De door straling geïnduceerde endotheliale dysfunctie, apoptose en senescentie kunnen leiden tot atherosclerose en uiteindelijk tot cardiovasculaire aandoeningen. In deze thesis werd er gefocust op stralingsgeïnduceerde senescentie in endotheelcellen en hun rol in de ontwikkeling van cardiovasculaire aandoeningen. Onze hypothese stelt dat ioniserende straling een senescent fenotype induceert in endotheelcellen, wat mogelijk beïnvloed kan worden door behandelingen met verschillende chemische stoffen.

Ten eerste werden drie verschillende testen uitgevoerd om senescentie vast te stellen in bestraalde primaire humane coronaire arterie endotheelcellen (HCAEC). De senescentie-geassocieerde  $\beta$ -galactosidase test die gebruik maakt van 5-bromo-4-chloro-3-indolyl- $\beta$ -D-galactopyranoside (X-gal) als substraat, wordt beschouwd als de gouden standaard. Deze standaard test werd vergeleken met de chlorophenol rood  $\beta$ -D-galactopyranoside (CPRG) en 4-methylumbelliferyl- $\beta$ -D-galactopyranoside (MUG) testen die een grotere verwerkingscapaciteit hebben. Er werd met alle drie de testen een hogere senescentie-geassocieerde  $\beta$ -galactosidase activiteit vastgesteld in 10 Gy bestraalde HCAEC op dag 6 na bestraling. De resultaten van de drie testen waren consistent, wat aantoont dat de CPRG en de MUG test goede alternatieven zijn voor de gouden standaard. Hierna werden de effecten van rosiglitazone, ascorbinezuur, insuline-achtige groeifactor-1 (IGF-1), hydrocortisone en atorvastatine op stralingsgeïnduceerde senescentie in HCAEC verder onderzocht met behulp van de CPRG en MUG testen. Behandeling met IGF-1 en hydrocortisone induceerde een hogere senescentie-geassocieerde  $\beta$ -galactosidase activiteit na 72 uur incubatie (zonder bestraling). Op dag 7 na bestraling met een dosis van 2 Gy was er een stijging te zien in de senescentie-geassocieerde  $\beta$ -galactosidase activiteit in de bestraalde onbehandelde HCAEC. Ook was er een significante stijging in senescentie-geassocieerde  $\beta$ -galactosidase activiteit in de rosiglitazone, IGF-1 en hydrocortisone-behandelde HCAEC vergeleken met de onbehandelde controles. Tot slot werd het effect van hydrocortisone behandeling op het stralingsgeïnduceerde senescent fenotype in HCAEC verder onderzocht door analyse van de eiwitexpressie en lokalisatie van p21, de stikstofoxide productie en de celgrootte. Western blot analyse toonde aan dat bestraling leidde tot verhoogde p21 hoeveelheden en behandeling met hydrocortisone resulteerde in een verlaging hiervan. De productie van stikstofoxide wordt verlaagd door hydrocortisone behandeling maar wordt niet beïnvloed of stijgt slechts licht door bestraling. Immunocytochemische kleuringen toonden aan dat er een significante stijging was in celgrootte, senescentie-geassocieerde  $\beta$ -galactosidase activiteit en p21 eiwitexpressie in de nuclei op dag 7 na bestraling.

Ioniserende straling kan dus gekoppeld worden aan vroegtijdige senescentie in endotheelcellen, hetgeen kan leiden tot atherosclerose. Er is echter meer onderzoek nodig om de onderliggende mechanismen te ontrafelen en om deze data aan te vullen met bewijs van andere senescentiemerkers. We hebben aangetoond dat behandeling met verschillende chemische stoffen stralingsgeïnduceerde senescentie in endotheelcellen kan beïnvloeden. Om de effecten van deze chemische stoffen op stralingsgeïnduceerde senescentie volledig te begrijpen en na te gaan of ze radioprotectief zijn, moeten ze verder bestudeerd worden in toekomstig *in vitro* en *in vivo* onderzoek. Het vinden van een chemische stof die bescherming biedt tegen stralingsgeïnduceerde senescentie in endotheelcellen zou het onderzoek naar radioprotectieve geneesmiddelen kunnen bevorderen.



## ABSTRACT

---

Cardiovascular disease is the most common cause of death worldwide and is in most cases the result of atherosclerosis. Risk factors for cardiovascular disease include behavioral factors, like smoking and physical inactivity, as well as non-modifiable factors like age and ethnicity. More recently, exposure to ionizing radiation was also identified as a risk factor for the development of cardiovascular disease based on epidemiological studies. Endothelial cells, lining the inner surface of the blood vessels, are believed to be the primary target of ionizing radiation-induced cardiovascular disease. Dysfunction, apoptosis and senescence of endothelial cells induced by ionizing radiation can trigger the process of atherosclerosis and eventually lead to cardiovascular disease. This thesis focusses on radiation-induced endothelial senescence and its role in cardiovascular disease. We hypothesized that ionizing radiation induces a senescent phenotype in endothelial cells, which could be modulated by treatment with various compounds.

First, three different assays were performed to detect senescence in irradiated primary human coronary artery endothelial cells (HCAECs). The senescence-associated  $\beta$ -galactosidase assay that uses 5-bromo-4-chloro-3-indolyl- $\beta$ -D-galactopyranoside (X-gal) as substrate is considered as the golden standard. This assay was compared with the chlorophenol red  $\beta$ -D-galactopyranoside (CPRG) and 4-methylumbelliferyl- $\beta$ -D-galactopyranoside (MUG) assays, which are high throughput alternatives for the standard assay. Higher senescence-associated  $\beta$ -galactosidase activity was observed in 10 Gy irradiated HCAECs at day 6 post-irradiation with all three assays. The results were consistent for all three assays, indicating that the CPRG and MUG assays are good alternatives for the golden standard. Next, the effects of rosiglitazone, ascorbic acid, insulin growth factor-1 (IGF-1), hydrocortisone and atorvastatin treatment on radiation-induced senescence in HCAECs was analyzed using the CPRG and MUG assays. Treatment with IGF-1 and hydrocortisone induced higher senescence-associated  $\beta$ -galactosidase activity after 72 hours. Irradiation with a dose of 2 Gy induced an increase in senescence-associated  $\beta$ -galactosidase activity in the untreated HCAECs at day 7 post-irradiation. Additionally, there was a significant increase in senescence-associated  $\beta$ -galactosidase activity in the rosiglitazone, IGF-1 and hydrocortisone-treated HCAECs compared to the untreated controls. Lastly, the effect of hydrocortisone treatment on the radiation-induced senescent phenotype of HCAECs was further investigated by analyzing p21 protein expression, nitric oxide production as well as cell size and p21 protein localization. Western blot analysis showed increased p21 expression induced by ionizing radiation and decreased expression by hydrocortisone treatment. The nitric oxide production was reduced by hydrocortisone treatment but unaffected or slightly increased by irradiation. Immunocytochemical staining showed increased cell size, senescence-associated  $\beta$ -galactosidase activity and p21 protein expression in the nucleus on day 7 post-irradiation.

Thus, our data suggest that ionizing radiation induces premature senescence in endothelial cells, which may trigger atherosclerosis. However, further research is necessary to elucidate the underlying mechanisms and to complement these data with additional evidence from other senescence markers. We showed that treatment with various compounds can modulate radiation-induced senescence in endothelial cells. These compounds could be the subject of future *in vitro* and *in vivo* research to fully understand their effects on radiation-induced senescence and to reveal their potential radioprotective character. Finding a compound that could protect against radiation-induced senescence of endothelial cells might benefit the research on radioprotective drugs.



# 1 INTRODUCTION

---

Cardiovascular disease (CVD) is the most common cause of death worldwide, accounting for 17.5 million deaths in 2012. 80% of the CVD mortality is due to coronary artery disease (42%) or stroke (38%) (Table S1), which are both caused by atherosclerosis. A lot of CVDs are the result of an unhealthy lifestyle and consequently could be prevented. Risk factors for CVD include unhealthy diet, smoking, excessive alcohol consumption and physical inactivity. These behavioral risk factors can lead to hypertension, high blood glucose levels, obesity and hypercholesterolemia, all increasing the cardiovascular risk (WHO, 2016a). However, CVDs are not always preventable because there are also risk factors that cannot be modified like family history, ethnicity, age,... (World Heart Federation, 2017). More recently, it was established that exposure to ionizing radiation is also a risk factor for the development of CVD. Because the use of medical procedures utilizing ionizing radiation is increasing rapidly, this risk factor has become a considerable concern for society (Reviewed in Adams *et al.*, 2003; Reviewed in Little *et al.*, 2008).

## 1.1 IONIZING RADIATION: A RISK FACTOR FOR CARDIOVASCULAR DISEASE

In the past, the heart was considered to be relatively resistant against damage induced by ionizing radiation. However, several epidemiological studies have been performed on populations who have been exposed to ionizing radiation due to nuclear accidents, occupation, diagnostics or radiotherapy. These studies have demonstrated that exposure to doses of ionizing radiation > 0.5 Gy is associated with the development of CVD, in contrary to the previous beliefs. For doses below 0.5 Gy, data are suggestive rather than persuasive due to the lack of statistical power and the presence of data confounders (Reviewed in Adams *et al.*, 2003; Reviewed in Little *et al.*, 2008; Lowe and Raj, 2014; Shimizu *et al.*, 2010).

### 1.1.1 Ionizing radiation

Radiation is defined as energy travelling through space. There are two types of radiation: non-ionizing radiation which carries low energy, for example sunlight or radiowaves, and ionizing radiation (World Nuclear Association, 2016). Ionizing radiation is a type of radiation that carries enough energy to ionize atoms. It consists of high energy electromagnetic waves (e.g.  $\gamma$ -rays, X-rays) or energetic particles (e.g.  $\alpha$ -particles,  $\beta$ -particles) moving at high speed. Ionizing radiation has been and still is extensively used in the industry as well as in the medical field. Examples of applications are sterilization of pharmaceuticals and food products, diagnostic tests and cancer therapy (Mehta, 2005). In addition, individuals are constantly exposed to ionizing radiation because of the natural background radiation, for example from cosmic rays or radioactive radon gas (Biddle, 2012).

Gamma- and X-ray radiation are both types of electromagnetic radiation and consist of short wavelength waves with high energy. The only difference between them is their origin. Gamma-rays originate from the nucleus, while X-rays derive from electrons in the outer shell of atoms (Mehta, 2005). X-rays can be generated using an X-ray tube by collision of accelerated electrons with metal atoms. During this process, the electron is slowed down or deflected when passing a nucleus of the metal atoms, thereby losing energy emitted as X-rays (the so-called 'bremsstrahlung'). Alternatively, it can eject an electron from the inner shell of the metal atom. A higher energy electron from the outer shell will replace the ejected electron with the concomitant emission of X-rays, called characteristic X-rays (Zink, 1997). Gamma-rays can emerge from radioisotopes, which are atoms with unstable nuclei. Radioisotopes will try to reach stability by either emitting a  $\alpha$ - or  $\beta$ -particle or by absorbing an electron in the nucleus followed by the emission of  $\gamma$ -rays. This characteristic of radioisotopes is called radioactivity. The resulting nucleus can be a stable isotope of another element but more frequently, the nucleus is in an excited state. When this is the case, it needs to lose energy in order to reach its stable state, which is the process of radioactive disintegration (Mehta, 2005). Because of their high energy,  $\gamma$ - and X-rays can deeply penetrate materials and consequently can also pass through the

human body. This can cause damage directly by interaction of the rays with biomolecules like DNA, proteins or lipids (Figure 1a). However, damage can also be induced indirectly when the rays interact with water molecules in the cells and induce the production of reactive oxygen species (ROS), for example hydroxyl radicals (OH<sup>\*</sup>) (Figure 1b) (Brenner and Hall, 2007; Murphy, 2009).

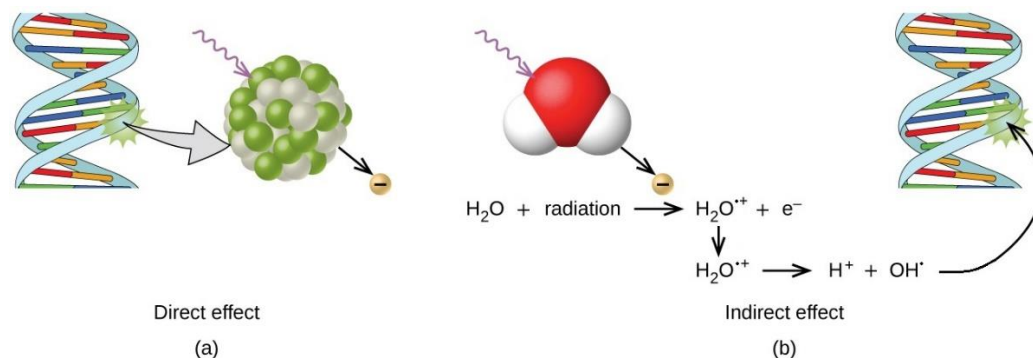


**Figure 1: Direct and indirect mechanisms of radiation-induced DNA damage** (Adapted from OpenStax Biology, 2016).

The unit of radioactivity is Becquerel (Bq). 1 Bq is defined as the occurrence of 1 disintegration per second within the source. However, when looking at biological effects, it is important to know the amount of radiation that is absorbed by the body and which could possibly cause damage. The absorbed dose is defined as the amount of energy, coming from any type of ionizing radiation, that is absorbed per unit mass of material. The international unit for absorbed dose is Gray (Gy). 1 Gy represents the absorption of 1 Joule of energy in 1 kilogram of mass (1 J/kg). To measure the biological effect, the type of radiation should also be taken into account because some types of radiation cause more harm than other types. An absorbed dose of  $\alpha$ -radiation is for example much more harmful than the same absorbed dose of  $\gamma$ -radiation. The equivalent dose comprises the absorbed dose as well as the type of radiation and is measured in Sievert (Sv) (Biddle, 2012; WHO, 2016b). It is calculated by multiplying the absorbed dose with the appropriate radiation weighting factor ( $W_R$ ). For X- and  $\gamma$ -rays this factor is 1, as a result 1 Gy is equivalent to 1 Sv (Figure S1). For higher energy types of radiation the weighting factors are higher, for example for  $\alpha$  particles the  $W_R$  is 20. Lastly, different organs and tissues have varying sensitivity to ionizing radiation. The effective dose includes these differences and represents the health risk for the entire body. It is defined as the sum of the equivalent doses for each tissue or organ multiplied by their tissue weighting factor ( $W_T$ ) (NEA OECD, 2011). For the heart, the tissue weighting factor is 0.12 (ICRP, 2007). Examples of effective doses associated with different sources of ionizing radiation are presented in Table 1.

**Table 1: The effective doses (mSv) associated with different sources of ionizing radiation** (Biddle, 2012; Fazel et al., 2009; Radiological Society of North America, 2016; UNSCEAR, 2000).

Source	Effective dose (mSv)	Time equivalent of exposure to natural background radiation (2.4 mSv/year)
Dental X-ray	0.005	1 day
Intercontinental flight per hour (depending on altitude)	0.001-0.01	4 hours - 1.5 days
Chest X-ray	0.1	12 days
Mammography	0.4	8 weeks
Computed tomography (CT) of the chest	7	2.5 years
Coronary CT angiography	12	5 years

With regard to the dose of radiation, a distinction can be made between low, moderate and high doses. Based on epidemiological studies on CVDs, dose ranges are defined as follows: < 0.5 Gy is considered a low dose, 0.5 Gy to 5 Gy is a moderate dose and doses > 5 Gy are high doses (Little *et al.*, 2008; Shimizu *et al.*, 2010).

### 1.1.2 Epidemiological evidence

The first epidemiological evidence indicating an increased risk of CVD was reported in the 1960s in patients treated for Hodgkin's disease (Fajardo and Stewart, 1970). It was observed that treatment with mediastinal radiotherapy led to a higher risk of coronary artery disease and myocardial infarction. Additionally, there was a higher risk of mortality observed from these cardiac events. The risk increased with time after exposure, which is in accordance with the slow progression of ionizing radiation-induced CVD that can take years or decades to develop (Figure 2A) (Boivin *et al.*, 1992; Hull *et al.*, 2003; Reinders *et al.*, 1999).

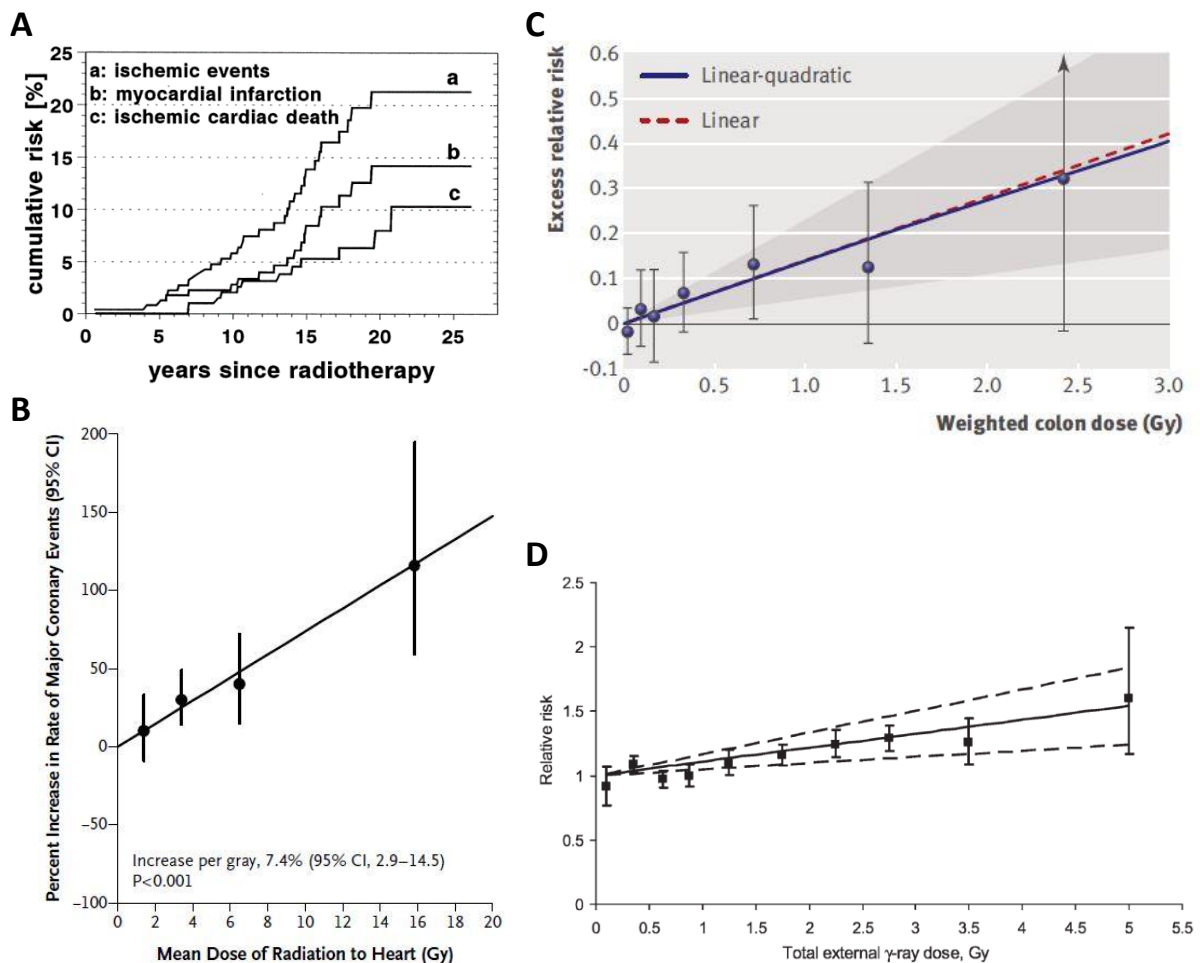


**Figure 2: Increase in risk of cardiovascular diseases after exposure to ionizing radiation.** A) Study performed on 258 patients with Hodgkin's disease, treated with radiotherapy who received a mean total X-ray dose of 36.6 Gy. Elevated risks of ischemic events (6.4% at 10 years to 21.2% at 20-25 years), myocardial infarction (3.4% at 10 years to 14.2% at 20-25 years) and ischemic cardiac mortality (2.6% at 10 years to 10.2% at 25 years) were observed (Reinders *et al.*, 1999). B) Study performed on 963 women treated with radiotherapy for breast cancer who received a mean total dose of 4.9 Gy to the heart. The rate of major coronary events is increased with 7.4% per Gy, without an apparent threshold (Darby *et al.*, 2013). C) Study on 86,611 Hiroshima and Nagasaki atomic bomb survivors with an estimated radiation dose between 0 and 4 Gy. An excess relative risk for death from heart disease of 14% per Gy was estimated. The linear model suggests risks even at low doses (Shimizu *et al.*, 2010). D) Study on 12210 Mayak workers who received a mean total  $\gamma$ -ray dose of 0.78 Gy. The incidence of ischemic heart disease is increased with an excess relative risk of 0.109 per Gy (Azizova *et al.*, 2010).

In 2007, a study on the Dutch Late Effects Breast Cancer Cohort (4,414 10-year survivors treated between 1970 and 1986) showed an elevated risk of myocardial infarction, angina pectoris and congestive heart failure in women who were treated with radiotherapy. Furthermore, the risk increased with time after exposure and was slightly higher, but remarkably not significant, for patients with left-sided breast cancer (Hooning *et al.*, 2007). A more recent study was performed by Darby *et al.* on breast cancer patients treated with radiotherapy between 1958 and 2001 in Sweden and Denmark. They found that the rate of ischemic heart disease increased by 7.4% per Gy increase of the mean dose to the heart, without an apparent threshold (Figure 2B). Additionally, they found significantly higher rates of ischemic heart disease in women irradiated for left-sided breast cancer as compared to patients who received radiotherapy for right-sided breast cancer. This observation is in accordance with the higher estimated mean dose to the heart of 6.6 Gy for women with left-sided breast cancer compared to an estimated mean dose of 2.9 Gy for women with right-sided breast cancer (Darby *et al.*, 2013).

The Life Span Study cohort is a population consisting of 86611 Hiroshima and Nagasaki atomic bomb survivors. The doses for the individuals included in this cohort were estimated based on the location and shielding at the time of the bombings. In this cohort, an elevated risk of CVD after exposure to a low dose of ionizing radiation was observed. The excess relative risk for stroke was estimated at 9% per Gy and at 14% per Gy for all heart diseases. A dose as low as 0.5 Gy already implicated an elevated risk, although the results were not significant for doses below 0.5 Gy (Figure 2C) (Shimizu *et al.*, 2010).

Another interesting population that can be used to study low dose radiation effects are the workers in the nuclear industry because they represent relatively large cohorts exposed to low levels of radiation and their radiation doses are well documented. In 2007, Vrijheid *et al.* performed a large-scale study on a 15-country nuclear workers cohort including 275,312 individuals exposed to an average cumulative dose of 20 mSv. In this study, there was an overall increasing trend of circulatory disease mortality, although not significant (Vrijheid *et al.*, 2007). However, several other studies on nuclear worker cohorts did find a significant correlation between exposure to low doses of radiation and the risk of CVDs and mortality. For example, a study was performed on a cohort of 12,210 Mayak workers who received a mean total dose of 0.78 Gy (Azizova *et al.*, 2010). The Mayak Production Association, producing plutonium-238 and tritium, was one of the largest nuclear facilities in Russia (Standing, 2006). In the Mayak worker cohort, a significant increase in ischemic heart disease incidence was observed with an excess relative risk of 0.109 per Gy (Figure 2D) (Azizova *et al.*, 2010). Also, a mortality study using the records of the National Dose Registry of Canada showed an increased risk of CVD mortality after occupational exposure to ionizing radiation. The estimated excess relative risk per 10 mSv of ionizing radiation exposure was 2.3% for males and 12.1% for females (Ashmore *et al.*, 1998). In 2000, Ivanov *et al.* performed a study on 68,309 Chernobyl liquidators of which the majority were exposed to ionizing radiation doses ranging from 0 to 200 mGy. They observed a significant increase in the incidence rate of circulatory diseases in relation to the radiation dose. Excess relative risks of 0.23 and 0.29 per Gy were identified for respectively the development of CVD and incidence of acute myocardial infarction (Ivanov *et al.*, 2000).

Because of the evidence mentioned above, an association between low doses (< 0.5 Gy) of ionizing radiation and excess risk of developing CVD is implied. However, these epidemiological studies should be interpreted with caution because other cardiovascular risk factors like age, smoking, hypertension and obesity (Glanzmann *et al.*, 1998; Vrijheid *et al.*, 2007) are all confounding factors that need to be corrected for, which is not always the case. In occupational exposure studies, the healthy worker survivor effect is another phenomenon that can introduce bias by masking the harmful effects of occupational exposure. Generally, the actively employed population has a lower mortality rate than the general population since severely ill and chronically disabled people are excluded from employment. Additionally, unhealthy workers are more likely to reduce their occupational exposure in contrast to the healthy workers who accumulate more exposure. Therefore, the healthy worker survivor effect poses a problem when studying occupational cohorts (Baillargeon, 2001; Picciotto *et*

*al.*, 2013; Shah, 2009). Furthermore, extremely large sample sizes are necessary to determine the risks of low doses of ionizing radiation with sufficient statistical precision and power. For example, to quantify the excess risk of a 10 mSv dose a cohort of approximately 5 million individuals is required, if the excess risk is proportional to the dose (Brenner *et al.*, 2003). As a consequence, radiobiological research is necessary to complement these epidemiological data with experimental evidence.

## 1.2 RADIATION-INDUCED CARDIOVASCULAR DISEASE

Radiotherapy has become one of the key elements in the treatment of cancer. It is estimated that 50% of the cancer patients are treated with radiotherapy. The prognosis of cancer patients was significantly improved by radiotherapy leading to an increased number of cancer survivors (Rodríguez, 2015; Yusuf *et al.*, 2011). However, late cardiovascular complications are often observed in these cancer survivors. The cumulative incidence of radiation-associated cardiotoxicity 5 to 10 years after radiotherapy is estimated to be 10 to 30% (Yusuf *et al.*, 2011). The last decades, radiotherapy techniques improved, lowering the exposure of the heart to ionizing radiation. Nevertheless, the risk of late cardiovascular effects after radiotherapy remains as the heart and its vessels still receive an incidental dose (Rodríguez, 2015; Yusuf *et al.*, 2011).

### 1.2.1 Atherosclerosis is the main cause of cardiovascular disease

The main cause of CVD worldwide is atherosclerosis, which can lead to ischemic heart disease, heart attack and stroke. Major risk factors for the development of atherosclerosis are for instance high blood pressure and high blood cholesterol, which can be caused by an unhealthy lifestyle including smoking, a lack of exercise and a bad diet (Herrington *et al.*, 2016). Atherosclerosis is characterized by the formation of plaques in the arteries, which is called atherogenesis (Figure 3). The process starts when qualitative changes occur in the layer of endothelial cells (ECs), that lines the inner surface of the arteries. When the ECs are exposed to irritative stimuli, for example pro-inflammatory agents, they will start to express adhesion molecules. These molecules make it possible for leukocytes to adhere to the EC surface. At the same time the endothelial permeability and composition of the extracellular matrix will change. This allows cholesterol-containing low-density lipoprotein (LDL) particles to enter the artery wall. Here, the LDL particles can become oxidized and may form aggregates. Next, chemoattractants will stimulate the entry of the attached leukocytes into the artery wall. The monocytes, which are the most abundant leukocyte type in plaques, will differentiate into tissue macrophages and start to take up the oxidized LDL particles. This will lead to intracellular cholesterol accumulation and transformation to foam cells. Production of pro-inflammatory agents by these foam cells will stimulate migration and proliferation of vascular smooth muscle cells (VSMCs). VSMCs produce extracellular matrix molecules, for example collagen and elastin, which will form a fibrous cap over the plaque. Accumulation of cellular debris and extracellular lipids underneath the fibrous cap will form the necrotic core of the plaque. The fibrous cap prevents exposure of the highly thrombogenic core to the blood. Plaques can lead to different types of clinical manifestations. For example, the plaque can keep on growing which will lead to a limitation of the blood flow and can cause tissue ischemia. When there is a disruption of the plaque, thrombi can be formed which can partially or completely occlude blood vessels leading to a heart attack or a stroke (Bentzon *et al.*, 2014; Libby *et al.*, 2011).

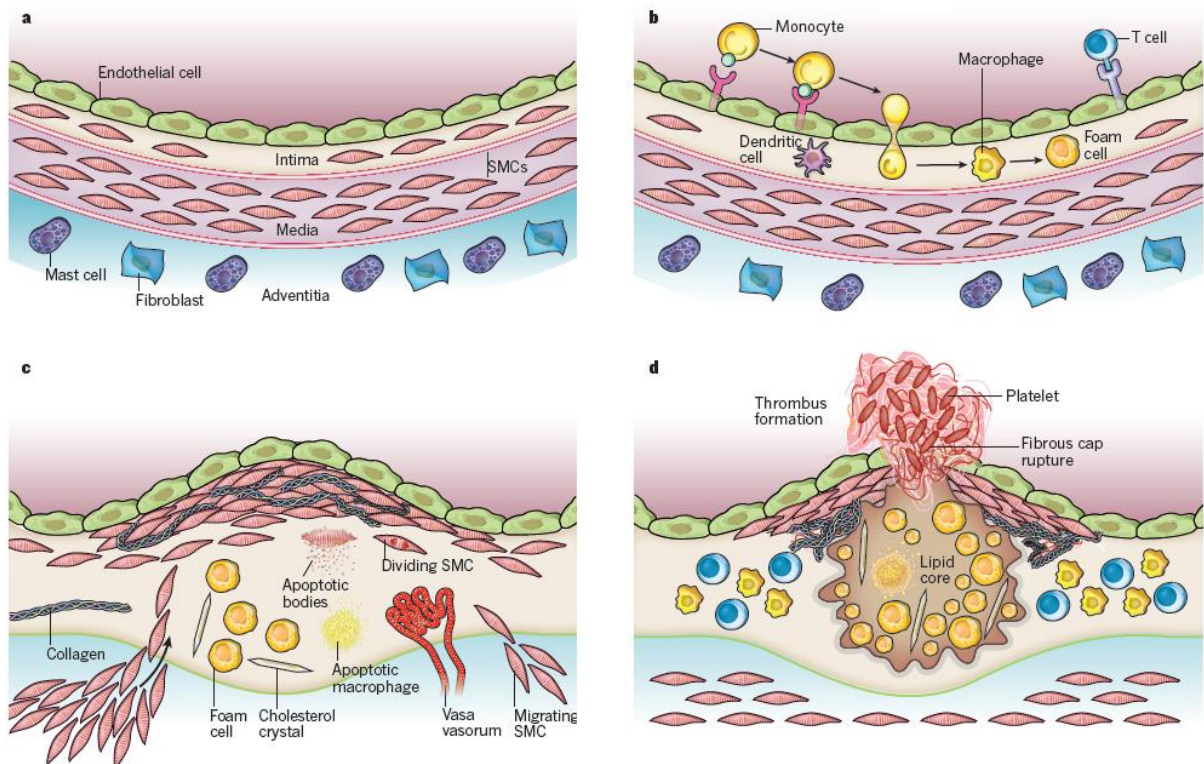


**Figure 3: Stages in the development of atherosclerotic lesions.** a) Composition of a normal artery wall. b) The first steps in the process of atherosclerosis include adhesion of monocytes (leukocytes) to the endothelium, migration of the monocytes into the artery wall, differentiation of monocytes into macrophages and take-up of LDL leading to formation of foam cells. c) VSMCs migrate, proliferate and start to produce extracellular matrix proteins. d) A necrotic core is formed by accumulation of cellular debris and extracellular lipids. Rupture of the plaque can lead to thrombosis (Libby *et al.*, 2011). (V)SMC: (vascular) smooth muscle cell, LDL: low-density lipoprotein

### 1.2.2 Pro-atherosclerotic effects of ionizing radiation

Ionizing radiation can contribute to the process of atherosclerosis in several ways. For example, ECs can die after interaction with ionizing radiation, thereby stimulating atherogenesis. This can occur through necrosis or apoptosis due to irreversible radiation damage (Reviewed in González, 1994; Reviewed in Schultz-Hector and Trott, 2007). Additionally, research has demonstrated that radiation can increase the expression of EC adhesion molecules like E-selectin, intercellular adhesion molecule (ICAM)-1 and platelet endothelial cell adhesion molecule (PECAM)-1, which play an important role in atherogenesis (Reviewed in Schultz-Hector and Trott, 2007). It has also been observed that EC irradiation leads to upregulation of pro-inflammatory cytokines, especially interleukin (IL)-6 and IL-8 (Baselet *et al.*, 2017; Reviewed in Schultz-Hector and Trott, 2007). Chronic inflammation stimulates the formation of a vulnerable atherosclerotic plaque. Furthermore, these pro-inflammatory effects can induce death in ECs, triggering atherogenesis. Besides the pro-inflammatory effects, radiation also has pro-thrombotic effects caused by an increased release of Von Willebrand factor by endothelial cells (Verheij *et al.*, 1994). Another effect of ionizing radiation is the induction of mutations, leading to genomic instability which is associated with the process of atherosclerosis (Reviewed in Schultz-Hector and Trott, 2007). As already mentioned earlier, radiation can damage DNA directly by ionization or indirectly through the formation of ROS (Brenner and Hall, 2007). Radiation-induced DNA damage and ROS production will increase the expression of the cell cycle inhibitor protein p21 and its regulator, tumor suppressor protein p53. This will activate the p53/p21 pathway, which induces premature senescence (Rombouts *et al.*, 2014; Yentrapalli *et al.*, 2013a; Yentrapalli *et al.*, 2013b). Dysfunction, apoptosis and senescence of ECs can eventually trigger the process of atherosclerosis (Busse and Fleming, 1996; Davignon and Ganz, 2004; Erusalimsky, 2009; Stoneman and Bennett, 2004).

### 1.3 RELEVANCE OF ENDOTHELIAL SENEESCENCE IN CARDIOVASCULAR DISEASE

As mentioned before, EC senescence can stimulate atherosclerosis causing CVD. Senescence is a cellular state of irreversible growth arrest and is associated with aging and age-related diseases. Senescent cells undergo distinctive changes in morphology, acquiring a flattened and enlarged cell shape. At the molecular level, senescent cells exhibit a specific gene expression pattern. The genes displaying altered expression include cell cycle regulatory genes, inflammation and stress-associated genes, cytoskeletal genes and metabolic genes. Senescent cells are permanently arrested in the G0/G1 phase of the cell cycle and are unresponsive to growth factors. However, they are still metabolically active which, in the case of senescent ECs, results in a pro-inflammatory, pro-atherosclerotic and pro-thrombotic phenotype and the expression of senescence-associated  $\beta$ -galactosidase activity at pH 6 (Erusalimsky, 2009; Kong *et al.*, 2011; Minamino and Komuro, 2007; Rombouts *et al.*, 2014).

#### 1.3.1 Mechanisms of cellular senescence

Cellular senescence was originally described by Hayflick and Moorhead in the 1960s. They observed senescence as a state in which cells cease to divide in culture after a certain amount of cell divisions and termed it 'replicative senescence' (Hayflick and Moorhead, 1961). Later on, it was discovered that telomeres, repetitive DNA sequences at the ends of chromosomes, play an important role in the induction of replicative senescence. Each cell division results in a gradual loss of telomeric DNA because conventional DNA polymerases are unable to replicate the very ends of linear chromosomes. Telomerase is an enzyme that is capable of synthesizing new telomeric repeats but is not expressed in most human somatic cells. When the telomeres reach a critical length, a DNA damage response will be triggered. This response will eventually lead to a permanent cell cycle arrest. Shortening of telomeres is not exclusively linked to the number of cell divisions but can also be influenced by other factors. For example, telomeres are very sensitive to oxidative damage and consequently, an increase in ROS will lead to accelerated telomere shortening. Furthermore, it has been observed that nitric oxide (NO) can

delay the shortening of telomeres and the induction of replicative senescence in ECs (Erusalimsky, 2009; Foreman and Tang, 2003; Kong *et al.*, 2011; Minamino and Komuro, 2007). On the other hand, senescence can also be triggered by a range of stress stimuli independent of telomere length and number of cell divisions. Examples are oxidative stress, DNA damage, inflammation, exposure to ionizing radiation and activated oncogenes like Rat Sarcoma (Ras). Senescence induced by one of these stimuli is referred to as 'stress-induced premature senescence'. Although the trigger is different, stress-induced premature senescence strongly resembles replicative senescence, for example in terms of morphology, expression of cell cycle regulators and senescence-associated  $\beta$ -galactosidase activity at pH 6 (Erusalimsky, 2009; Itahana *et al.*, 2001; Kong *et al.*, 2011; Kuilman *et al.*, 2010; Rombouts *et al.*, 2014).

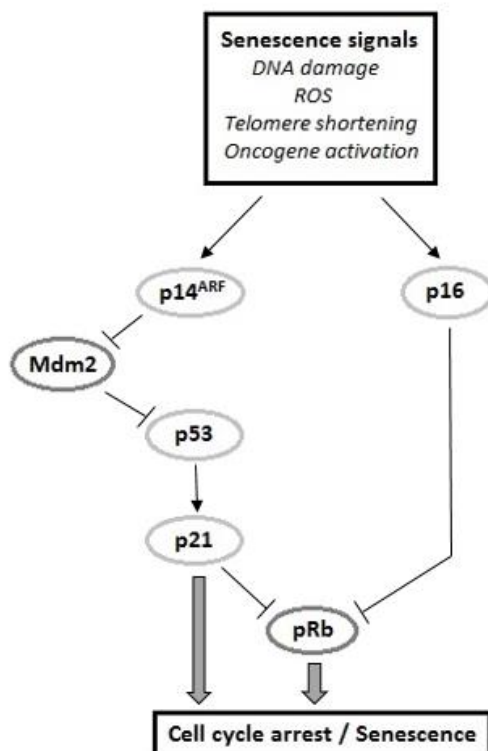


Figure 4: Pathways involved in the induction of senescence (Chen *et al.*, 2006).

Despite the fact that senescence can be induced by different stimuli, ultimately these senescence-inducing signals all activate the p53/p21 and/or p16/retinoblastoma protein (pRb) pathways (Figure 4). P53 is a transcriptional regulator that plays a crucial role in the DNA damage response. The presence of DNA damage will activate ataxia-telangiectasia mutated/ataxia-telangiectasia and Rad3 related

(ATM/ATR) kinases and checkpoint kinase 1 and 2 (Chk1/Chk2), which will phosphorylate p53. This will lead to stabilization and activation of p53. Overexpression of p14<sup>ARF</sup> is another event that can lead to stabilization and activation of p53. P14<sup>ARF</sup> is a tumor suppressor protein that is upregulated in senescent cells. It can bind to Mouse double minute 2 (Mdm2), an E3 ubiquitin ligase, which normally targets p53 for ubiquitylation and degradation by the proteasome. However, binding of p14<sup>ARF</sup> to Mdm2 will inhibit its function, leading to stabilization and activation of p53. One of the main target genes of p53 is the cyclin-dependent kinase inhibitor p21. The expression of p21 has shown to be upregulated in senescent cells. The increased expression of p21 will lead to inhibition of pRb phosphorylation, which is necessary for cell cycle progression. Thus, in the end, overexpression of p21 induces a cell cycle arrest. P16 is another cyclin-dependent kinase inhibitor that shows increased expression in senescent cells. It is hypothesized that p16 is necessary to maintain the senescent cellular state. Just like p21, overexpression of p16 will cause hypophosphorylation of pRb, leading to cell cycle arrest (Itahana *et al.*, 2001; Kong *et al.*, 2011; Minamino and Komuro, 2007).

### 1.3.2 Senescent endothelial cells play a role in cardiovascular disease

The endothelium is the main regulator of vascular homeostasis. It regulates the vascular tone by maintaining the balance between vasodilation and vasoconstriction. This is accomplished through the release of vasodilative (e.g. NO), and vasoconstrictive substances (e.g. angiotensin II) by ECs. Furthermore, the endothelium regulates VSMC proliferation and migration as well as the balance between thrombogenesis and fibrinolysis. Lastly, the endothelium exerts an anti-inflammatory function. Hence, a good functioning endothelium is crucial for vascular health. Damage to the endothelium or endothelial dysfunction, e.g. caused by senescence, will initiate processes that will stimulate atherosclerosis (Davignon and Ganz, 2004).

It has been demonstrated that senescent ECs are present in atherosclerotic plaques in human coronary arteries (Minamino *et al.*, 2002). Senescent ECs can contribute to the development of CVDs in several ways (Figure 5). First of all, the permanent proliferation arrest of senescent ECs may affect the repair capacity of the endothelium. However, EC senescence is not only characterized by a replication arrest but also by changes in gene expression, function and morphology. For example, the expression of proteins associated with cytoskeletal function and cellular architecture is altered in senescent ECs. Because of these changes, the motility of the ECs is impaired thereby reducing the angiogenic capacity. Additionally, ECs undergoing senescence overexpress pro-inflammatory proteins like IL-1 $\alpha$  and ICAM-1 and pro-thrombotic proteins like plasminogen activator inhibitor-1 (PAI-1). Furthermore, it has been observed that senescent ECs degrade less atherogenic lipoproteins as compared to non-senescent ECs. The accumulation of atherogenic lipoproteins promotes the formation of atherosclerotic plaques. There is also evidence from several studies that there are lower levels of endothelial nitric oxide synthase (eNOS) activity in senescent ECs and that the production of NO is reduced. As a result, the bioavailability of NO, which is critical for normal endothelial function, will be decreased. In senescent EC cultures the levels of the important vasodilator prostacyclin were also reduced. *In vivo*, this reduction would lead to an imbalance in vascular tone. Lastly, another important player in atherogenesis and consequently in the development of CVD, is the level of ROS. Senescent ECs produce more ROS than non-senescent ECs, thereby promoting atherogenesis. All the above mentioned phenotypic changes will have pathophysiological consequences such as reduced angiogenesis and vasodilatation, increased vascular inflammation and stimulation of atherogenesis and thrombosis. In the end, all these effects may lead to the development of CVD (Reviewed in Erusalimsky, 2009).

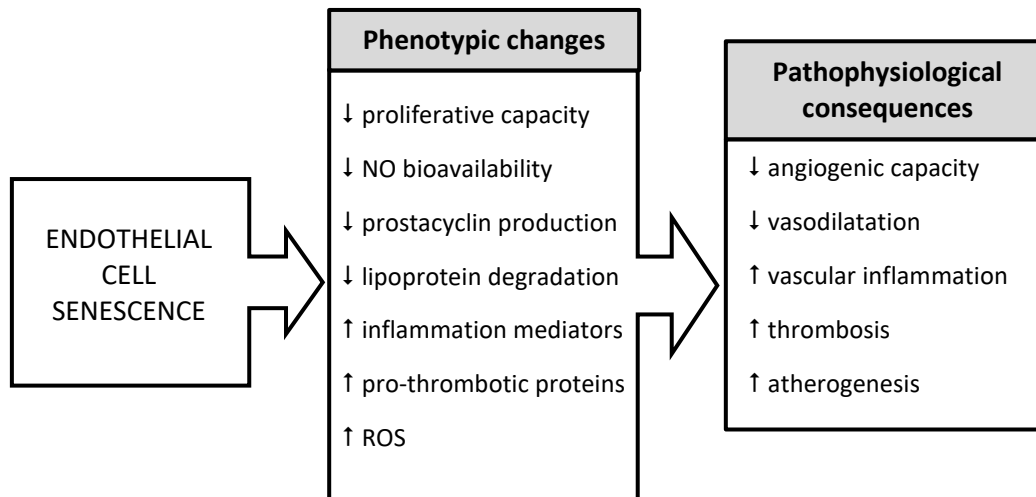


**Figure 5: Phenotypic changes in senescent endothelial cells and their pathophysiological consequences** (Adapted from Erusalimsky, 2009). NO: nitric oxide, ROS: reactive oxygen species.

### 1.3.3 Biomarker for the identification of senescent cells

In the past, it was impossible to differentiate between senescent cells and quiescent cells or terminally differentiated cells, which made research on senescence and its mechanisms very difficult. However, in 1995 Dimri *et al.* reported that  $\beta$ -galactosidase ( $\beta$ -gal) activity at a pH of 6 is a biomarker for senescence in human cells. Non-senescent cells express optimal lysosomal  $\beta$ -gal activity at an acidic pH of 4 to 4.5 but considerably lower activity at a pH of 6. Therefore, it is only detectable at acidic pH in proliferating cells and not at pH 6. At the time, it was not clear whether the senescence-associated  $\beta$ -galactosidase (SA  $\beta$ -gal) activity was of lysosomal origin (Dimri *et al.*, 1995). Later on, in 2006, Lee *et al.* demonstrated that the SA  $\beta$ -gal activity is expressed from the galactosidase beta 1 gene, which is the gene encoding the lysosomal  $\beta$ -gal. Furthermore, they observed that the protein levels of the lysosomal  $\beta$ -gal increase during senescence. This led to the suggestion that the increase in lysosomal  $\beta$ -gal activity in senescent cells is sufficient to pass the threshold for detection at pH 6.0. However, the increase in lysosomal  $\beta$ -gal protein levels is not proportional to the increase in  $\beta$ -gal activity detected at pH 6.0 in senescent cells. Hence, the high SA  $\beta$ -gal activity in senescent cells is not solely caused by the increase in protein levels and there must be additional functional differences in senescent lysosomes or other factors that contribute to the increase in SA  $\beta$ -gal activity (Lee *et al.*, 2006).

## 1.4 CANDIDATE MODULATORS OF PREMATURE SENESENCE

### 1.4.1 IGF-1

Insulin-like growth factor-1 (IGF-1) is a protein that plays a critical role in several cellular processes, including the regulation of cellular growth and proliferation (Handayaningsih *et al.*, 2012; Takahashi, 2012; Tran *et al.*, 2014). It is produced in response to growth hormone stimulation and secreted in the blood, mainly by hepatocytes (Takahashi, 2012). Increased IGF-1 signaling is associated with induction of cell proliferation and survival by activation of the IGF-1 receptor (IGF1R), which leads to upregulation of the phosphatidylinositol 3-kinase (PI3K)/Akt pathway. However, it is also known that disruption of IGF-1 signaling can enhance longevity and delay aging processes (Takahashi, 2012; Tran *et al.*, 2014). IGF binding proteins (IGFBPs) play an important role in IGF signaling by modulation of IGF bioavailability. IGFBPs belong to a family of proteins that bind IGF-1 and IGF-2 with high affinity. Binding of IGF-1 to IGFBPs limits the binding to the IGF1R, thereby inhibiting IGF-1 action (Reviewed in Baxter, 2000; Kim *et al.*, 2007). However, there is also evidence of a potentiation effect on IGF activity exerted by binding of IGF to IGFBP1, 3 and 5 although the involved mechanisms are still unknown (Reviewed in Baxter, 2000).

Recently, Tran *et al.* demonstrated that IGF-1 can promote cell proliferation as well as cellular senescence, revealing a dual function for IGF-1. They showed that acute IGF-1 signaling stimulates cell proliferation, which can be counteracted by p53. On the other hand, prolonged IGF-1 exposure can induce premature senescence in a p53-dependent way. Previously, it has been reported that deacetylase sirtuin 1 (SIRT1) plays an important role in cellular senescence and that SIRT1 can deacetylate and inactivate p53. Now, there is evidence that prolonged IGF-1 treatment inhibits SIRT1 activity, leading to increased p53 acetylation and thereby stabilization and activation of p53. This will ultimately result in the induction of premature senescence (Tran *et al.*, 2014).

Enhancement of cellular senescence by IGF-1 was also reported by Handayaningsih *et al.* They also showed that the expression of p53 and p21, which are both associated with senescence, was increased by IGF-1 stimulation. Therefore, they suggested that the induction of premature senescence by IGF-1 is p53-dependent, consistent with the findings of Tran and colleagues. Additionally, they found that ROS play a role in the induction of senescence by IGF-1 (Handayaningsih *et al.*, 2012).

There is also evidence that the IGFBPs are involved in premature senescence. It has been reported that the expression of IGFBP3 and 5 is increased in senescent ECs (Hampel *et al.*, 2006). Kim *et al.* showed that IGFBP5 can accelerate senescence in young human umbilical vein endothelial cells (HUVECs) through a p53-dependent mechanism. Also, immunohistochemical staining revealed that atherosclerotic plaques are strongly positive for IGFBP5 (Kim *et al.*, 2007). Moreover, the expression of IGFBP5 was shown to be upregulated in irradiated HUVECs from week 3 onwards after irradiation. This increase in expression could be related to inactivation of the PI3K/Akt/mammalian target of rapamycin (mTOR) pathway. It is suggested that the inactivation of this pathway is involved in the induction of premature senescence in ECs after irradiation (Rombouts *et al.*, 2014; Yentrapalli *et al.*, 2013b). Lastly, increased SA  $\beta$ -gal activity and secretion of IGFBP7 has been reported in irradiated telomerase-immortalized coronary artery endothelial cells (TICAE) on day 14 after irradiation (Baselet *et al.*, 2017).

The evidence mentioned above is summarized in Figure 6 and suggests a role for IGF-1 and its binding proteins in premature senescence. Therefore, it would be interesting to further elucidate whether IGF-1 also has an effect on the process of radiation-induced premature senescence.

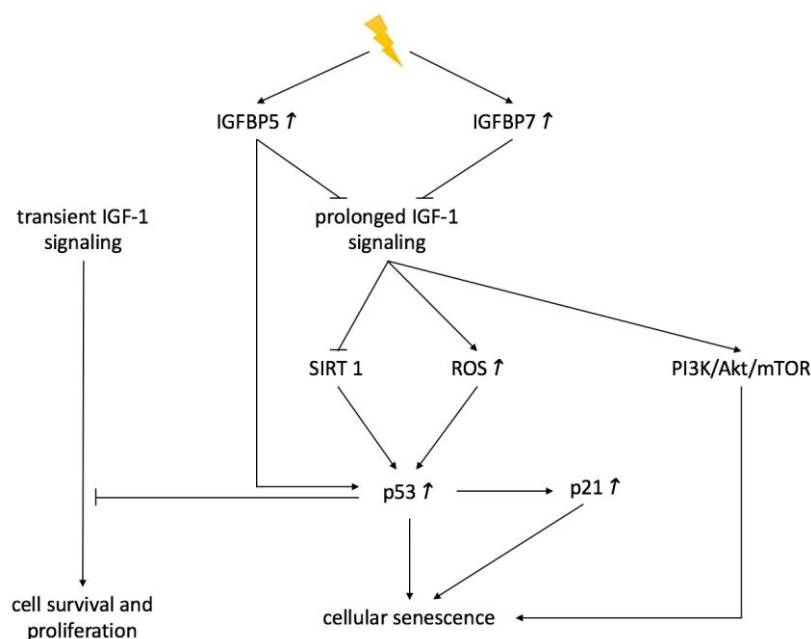


**Figure 6: Summary of the effects induced by insulin-like growth factor-1 signaling.** IGF-1: insulin-like growth factor-1, IGFBP: insulin-like growth factor binding protein, mTOR: mammalian target of rapamycin, PI3K: phosphatidylinositol 3-kinase, ROS: reactive oxygen species, SIRT 1: sirtuin 1.

### 1.4.2 Statins

Statins are drugs that are used to manage and prevent CVDs and are one of the most prescribed drugs worldwide. Statins bind to 3-hydroxy-3-methyl-glutaryl-coenzyme A (HMG-CoA) reductase, an enzyme from the mevalonate pathway. The binding will inhibit this pathway and consequently stop the biosynthesis of cholesterol and isoprenoids like geranylgeranyl pyrophosphate and farnesyl pyrophosphate. These isoprenoids are used for the process of isoprenylation, which is the attachment of lipids to several cell signaling proteins. This process is essential for the activation and intracellular transport of the signaling proteins. Acting as molecular switches, the signaling proteins control different pathways and cell functions like motility, differentiation and proliferation. This indicates that statins also have other effects besides the lowering of cholesterol levels, which are called pleiotropic effects. These effects include for example improvement of endothelial function and stabilization of atherosclerotic plaques (Gazzerro *et al.*, 2012). Furthermore, there is evidence that statins have a radioprotective effect. They can reduce ionizing radiation-induced expression of pro-inflammatory and pro-fibrotic cytokines *in vivo* in 6 Gy irradiated mice (Reviewed in Fritz *et al.*, 2011; Ostrau *et al.*, 2009). Furthermore, it was observed that lovastatin can prevent radiation-induced apoptosis of HUVECs after  $\gamma$ -irradiation with a dose of 10 Gy, possibly by inhibition of pro-apoptotic mechanisms regulated by p53 (Nubel *et al.*, 2006).

Atorvastatin is one of the most popular types of statins (Roland, 2015). It is a lipophilic component which enables it to enter cells by passive diffusion. Additionally, it is an open acid statin, which is the active form of statins. This means that it doesn't have to be hydrolyzed in the body before becoming active. Compared to other statins like lovastatin, pravastatin and simvastatin, atorvastatin has a long half-life of 11 to 30 hours (Gazzerro *et al.*, 2012). A normal dose of atorvastatin is 40 mg per day, but it can be increased to a dose of 80 mg per day. These doses are consistent with plasma concentrations of 20-30 ng/ml and 40-70 ng/ml, respectively (Gazzerro *et al.*, 2012; Lins *et al.*, 2003; Roland, 2015).

As already known, statins can be used to prevent or manage CVDs. Atorvastatin can act through different mechanisms to achieve this. First of all, high cholesterol levels are a major risk factor for CVD. Atorvastatin is capable of lowering these levels, thereby reducing the risk of CVD. Furthermore, it has been observed that atorvastatin reduces the expression of adhesion molecules, like ICAM-1 and vascular cell adhesion molecule (VCAM)-1, on ECs. This will result in reduced infiltration of leukocytes into the vascular wall during the process of atherogenesis. Additionally, atorvastatin can reduce inflammation by inhibition of pro-inflammatory cytokine production. Wang *et al.* showed for example that atorvastatin significantly reduced the expression of IL-6, IL-1, transforming growth factor- $\beta$  (TGF- $\beta$ ) and some other cytokines and chemokines. Atorvastatin can also reduce endothelial dysfunction by increasing the NO availability and preventing the formation of ROS. Furthermore, Schmidt-Lucke *et al.* found that atorvastatin can inhibit apoptosis of ECs (Reviewed in Gazzerro *et al.*, 2012).

Aside from the mechanisms discussed above, atorvastatin can also influence the development of CVDs by prevention of EC senescence. Previous research has shown that atorvastatin can regulate the expression of various cell cycle regulatory proteins, including p27, via the PI3K pathway in endothelial progenitor cells. It is suggested that reduced expression of the cell cycle inhibitory protein p27 and an increase in cell cycle promoting proteins might prevent the onset of replicative senescence (Assmus *et al.*, 2003). Also, it has been demonstrated that atorvastatin increases the phosphorylation of Akt in ECs, which leads to activation of the PI3K/Akt pathway. This activation induces increased eNOS expression and ultimately increases the expression of the longevity gene, SIRT1. Further research showed that eNOS and SIRT1 closely interact to inhibit senescence in ECs (Ota *et al.*, 2010). All the effects induced by atorvastatin are summarized in Figure 7. However, the effect of atorvastatin on radiation-induced senescence in ECs still needs to be further elucidated.

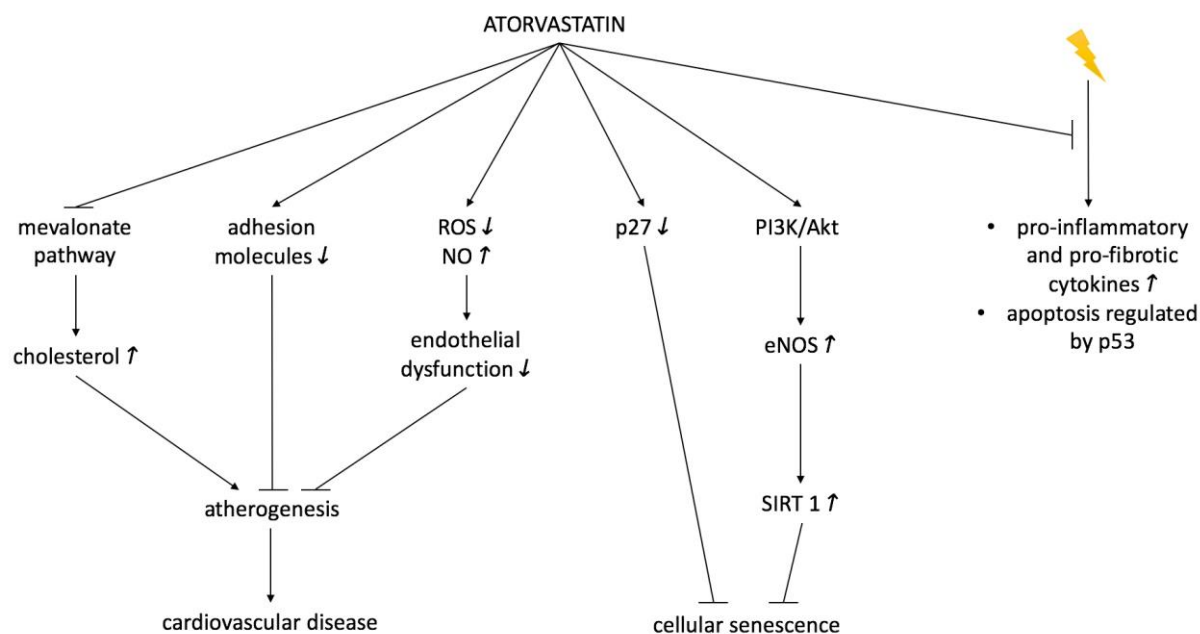


**Figure 7: Summary of the effects induced by atorvastatin.** eNOS: endothelial nitric oxide synthase, NO: nitric oxide, PI3K: phosphatidylinositol 3-kinase, ROS: reactive oxygen species, SIRT 1: sirtuin 1.

### 1.4.3 Ascorbic acid

Ascorbic acid (ASC) is a naturally occurring organic compound with antioxidant characteristics. It is one of the many forms, so-called vitamers, of vitamin C. Humans are not capable of synthesizing vitamin C, therefore it must be provided by the diet (Montecinos *et al.*, 2007). However, due to its water solubility and sensitivity to oxygen, it can be partially destroyed during food processing. A deficiency of vitamin C can for instance cause microcytic anemia and ultimately, in case of a serious deficiency, to scurvy (José Luis Silencio Barrita, 2013).

ASC plays several important roles in the body. First of all, it is a cofactor for several enzymes. For example, it is necessary for the synthesis of collagen, which is present in several connective tissues in the body like bone, cartilage, blood vessels and heart valves. Additionally, ASC is required for the synthesis of hormones, e.g. oxytocin, and neurotransmitters like dopamine. It is also involved in the metabolism of amino acids and other vitamins. However, ASC is mainly known and used for its antioxidant features. It can significantly decrease the adverse effects of ROS by donating an electron, thereby reducing them. ASC can also act as a co-antioxidant by regeneration of the antioxidant alpha tocopherol (vitamin E) (José Luis Silencio Barrita, 2013; Naidu, 2003).

ASC can also play a role in the development and maintenance of CVDs. Epidemiological studies have indicated that ASC can reduce the incidence of mortality from heart diseases and stroke. However, the evidence for a possible protective effect on CVD is inconclusive (José Luis Silencio Barrita, 2013; Naidu, 2003). Additionally, it is involved in the catabolism of cholesterol in the liver and prevents hypercholesterolemia. Furthermore, its antioxidant characteristics prevent lipid peroxidation and oxidation of LDL, which are associated with the formation of atherosclerotic plaques. *In vivo* studies have also shown that ASC can inhibit leukocyte-endothelial cell interactions, which is also an important step in atherogenesis (Naidu, 2003).

Antioxidants in general can reduce the formation of intracellular ROS, thereby delaying senescence in endothelial cells (Haendeler *et al.*, 2004). A more recent study showed that the delayed increase in ROS after irradiation with an X-ray dose of 0.5 to 4 Gy can be suppressed by treatment with ASC, which led to reduced induction of senescence in mammalian fibroblast cells (Kobashigawa *et al.*, 2015). This leads to the hypothesis that AA may have an effect on radiation-induced senescence in endothelial cells.

#### 1.4.4 Hydrocortisone

Hydrocortisone, also named cortisol, is a hormone belonging to the family of corticosteroids, more specifically to the subclass of glucocorticoids. In the body, glucocorticoids mainly play a role in the regulation of metabolic processes. However, they can also exert effects on for example the cardiovascular and the immune system. Hydrocortisone induces these effects by activating the glucocorticoid receptor (GR) in target tissues, leading to an alteration in the expression of corticosteroid-responsive genes. Today, corticosteroids are most commonly used as an anti-inflammatory drug (Spoelhof and Ray, 2014).

The anti-inflammatory function of hydrocortisone can have implications in the process of atherosclerosis. One of the anti-inflammatory mechanisms of hydrocortisone and other corticosteroids, is the modulation of leukocyte-adhesion to the vascular endothelium. Cronstein *et al.* showed that cortisol can inhibit the expression of adhesion molecules, for example ICAM-1. This prevents the recruitment and infiltration of leukocytes into the vascular wall, which is a key step in the development of atherosclerotic plaques (Cronstein *et al.*, 1992; Libby *et al.*, 2011).

Besides the anti-inflammatory function of hydrocortisone, there are several reports that illustrate the effect of hydrocortisone on cell proliferation and lifespan. For example, there is evidence that addition of hydrocortisone to the culture medium increases the proliferation and replicative lifespan of human fetal lung fibroblasts (Ban *et al.*, 1980; Cristofalo and Rosner, 1979; Kondo *et al.*, 1983). These observations implicate that hydrocortisone is capable of modulating the transition of cells to a less actively proliferating state. This hypothesis is also supported by the observation that hydrocortisone treatment delays the lengthening of the G<sub>1</sub> phase, which is a normal phenomenon in ageing cells. Additionally, hydrocortisone can stimulate entry into the S phase and can initiate DNA synthesis in cells that would normally not initiate DNA synthesis (Cristofalo and Rosner, 1979; Phillips *et al.*, 1982). Because hydrocortisone has an effect on the proliferation capacity and can delay the onset and rate of senescent changes in human fetal lung fibroblasts (Cristofalo *et al.*, 1985), it would also be interesting to check whether hydrocortisone has an effect on radiation-induced senescence in ECs.

#### 1.4.5 Rosiglitazone

Rosiglitazone (Avandia®; GlaxoSmithKline) is a drug that belongs to the class of thiazolidinediones (TZD). It is used for the treatment of type 2 diabetes because it lowers the blood glucose levels by increasing insulin sensitivity. This effect is achieved by TZD acting as agonists for the peroxisome-proliferator-activated receptor gamma (PPAR-γ). The PPAR-γ receptor is a ligand-activated nuclear transcription factor that modulates the expression of genes involved in glucose and insulin homeostasis, lipid metabolism and cellular differentiation (Lombardi *et al.*, 2008; Nissen and Wolski, 2007). Although rosiglitazone has the ability to efficiently reduce blood glucose levels in type 2 diabetes, it was withdrawn from the European market in 2010 because of its adverse effects on the heart (European Medicines Agency, 2016). Several studies indicated that rosiglitazone significantly increases the risk of heart failure and myocardial infarction but despite the increase in cardiovascular morbidity, the risk of cardiovascular mortality is not increased (Home *et al.*, 2009; Nissen and Wolski, 2007; Singh *et al.*, 2007). This led to the withdrawal by the European Medicines Agency because the benefits of the drug did not outweigh the risks anymore. On the contrary, rosiglitazone is still available on the market in the USA. The FDA restricted the use of rosiglitazone in 2010 and started an investigation on the cardiovascular risks of the drug. In 2013, the restrictions were abrogated because

research showed no increased risk of heart attack after treatment with rosiglitazone compared to the standard type 2 diabetes medicines metformin and sulfonylurea (FDA, 2015).

Even though there are reports that rosiglitazone can increase the risk of heart failure and myocardial infarction, there is also evidence that rosiglitazone can have a positive effect and prevent the development of CVDs. For example, the levels of C-reactive protein, matrix metalloproteinase-9 and white blood cells, which are inflammation markers and risk factors for CVD, are reduced by treatment with rosiglitazone (Haffner *et al.*, 2002). This anti-inflammatory effect of rosiglitazone was also seen by Marx *et al.* They showed that PPAR- $\gamma$  agonists, like rosiglitazone and pioglitazone, reduce the production of the pro-inflammatory cytokines interferon- $\gamma$  (IFN- $\gamma$ ), tumor necrosis factor- $\alpha$  (TNF- $\alpha$ ) and IL-2 by T lymphocytes. Activation of T lymphocytes and subsequent production of inflammatory cytokines is an important step in atherosclerotic plaque development (Marx *et al.*, 2002). More recently, Lombardi *et al.* showed that the anti-inflammatory action of PPAR- $\gamma$  agonists, like rosiglitazone, is due to the inhibition of the pro-inflammatory transcription factor nuclear factor kappa B (NF- $\kappa$ B). They also showed that rosiglitazone can interfere with chemokine secretion stimulated by TNF- $\alpha$  and IFN- $\gamma$  in microvascular endothelial cells. Additionally, the expression of VCAM-1 and ICAM-1 by human microvascular endothelial cells was reduced by rosiglitazone treatment (Lombardi *et al.*, 2008). Both chemokine secretion and expression of adhesion molecules are important steps in the development of an atherosclerotic plaque (Libby *et al.*, 2011; Lombardi *et al.*, 2008).

Other studies revealed that PPAR- $\gamma$  activity is also involved in the regulation of oxidative stress. For example, treatment with a PPAR- $\gamma$  agonist or overexpression of PPAR- $\gamma$  can reduce the ROS production induced by ultraviolet A (UVA) radiation or ageing in human dermal fibroblasts in culture (Briganti *et al.*, 2014; Lee *et al.*, 2010). Furthermore, endogenous antioxidants and the total antioxidant capacity are increased by treatment with a PPAR- $\gamma$  agonist (Briganti *et al.*, 2014). Oxidative stress plays an important role in stress-induced premature senescence. Therefore, the role of PPAR- $\gamma$  agonists, like rosiglitazone, in the premature senescence process was also investigated. Evidence was found that rosiglitazone can reduce the proportion of senescent fibroblasts after exposure to ultraviolet B (UVB) radiation (Chen *et al.*, 2015). Also, after exposure to UVA radiation, modulation of PPAR- $\gamma$  activity with the agonist Octa can rescue the senescent phenotype in fibroblasts (Briganti *et al.*, 2014). Lastly, modifying the PPAR- $\gamma$  activity with rosiglitazone can counteract UVB radiation-induced upregulation of p53 and p21, which are both associated with senescence (Chen *et al.*, 2015). Further research is necessary to determine the effect of rosiglitazone on ionizing radiation-induced senescence in endothelial cells.

## 1.5 RESEARCH AIMS AND OBJECTIVES

The aim of this thesis is to study the effect of the candidate modulators mentioned above on radiation-induced senescence in endothelial cells. First of all, three different assays will be performed to detect radiation-induced senescence in endothelial cells. The SA  $\beta$ -gal assay that uses 5-bromo-4-chloro-3-indolyl- $\beta$ -D-galactopyranoside (X-gal) as substrate is considered as the golden standard assay. The chlorophenol red  $\beta$ -D-galactopyranoside (CPRG) and 4-methylumbelliferyl- $\beta$ -D-galactopyranoside (MUG) assay are high throughput alternatives for the standard assay. Next, the CPRG and MUG assays will be used to determine the effects of the different compounds on radiation-induced senescence in endothelial cells. Additionally, western blot analysis will be performed to study the effects on p21 and p16 protein expression. Lastly, the nitric oxide production will be examined in irradiated endothelial cells and immunocytochemical stainings will be performed to study cell size, SA  $\beta$ -gal activity as well as p21 protein expression and localization.

## 2 MATERIALS AND METHODS

---

### 2.1 CELL CULTURE

Primary human coronary artery endothelial cells (HCAECs, ATCC PCS-100-020, France) were used for all experiments. The cells were cultured in Vascular Cell Basal Medium (ATCC PCS-100-030, France) supplemented with the Endothelial Cell Growth Kit-VEGF (ATCC PCS-100-041, France) in a humidified incubator at 37°C with 5% CO<sub>2</sub>. 72 hours before irradiation, treatment with one of the following compounds was started: rosiglitazone 1 μM (Sigma-Aldrich, Overijse, Belgium), ascorbic acid 1 mM (ATCC PCS-100-041, France), IGF-1 100 ng/ml (ATCC PCS-100-041, France), hydrocortisone hemisuccinate 100 ng/ml (ATCC PCS-100-041, France), or atorvastatin calcium salt trihydrate 0.4 nM (Sigma-Aldrich, Overijse, Belgium). All compounds were added to Vascular Cell Basal Medium containing the Endothelial Cell Growth Kit-VEGF without hydrocortisone hemisuccinate.

### 2.2 IRRADIATION

Cells were irradiated with a dose rate of 0.5 Gy/min, using an Xstrahl RX generator (250 kV, 12 mA, 3.8 mm Al and 1.4 mm Cu; Camberley). Doses applied were 2 or 10 Gy. Cells were not passaged during the experiment.

### 2.3 STANDARD SENESENCE-ASSOCIATED B-GALACTOSIDASE ASSAY

The cells were seeded in a 96-well plate at 10,000 cells per well. The senescence-associated β-galactosidase (SA β-gal) activity was determined at various time points using a histochemical senescence detection kit (ab65351) according to the manufacturer's instructions (Abcam, Cambridge, UK). Briefly, the cells were washed with 1x phosphate buffered saline (PBS), fixed with the 1x Fixative Solution for 10-15 minutes at room temperature and washed again with 1x PBS. Next, the cells were incubated with the SA β-gal staining solution at 37°C for 18 h without CO<sub>2</sub>. The staining solution contains the X-gal substrate, which will form an insoluble blue compound when cleaved by β-galactosidase. The SA β-gal staining reaction was stopped by addition of 1 M Na<sub>2</sub>CO<sub>3</sub>. The cells were counterstained using Giemsa staining (VWR, Leuven, Belgium) acidified by 1:50 dilution in 0.2 M sodium acetate buffer pH 3.36. Using light microscopy, the percentage of SA β-gal blue stained cells was determined by manually counting a minimum of 1,000 cells and checking the presence of blue color. Nuclei were stained with 4',6-diamidino-2-phenylindole (DAPI) to determine the number of cells per well using ImageJ software.

### 2.4 CPRG ASSAY

The cells were seeded in a 96-well plate at 10,000 cells per well. At various time points after irradiation, the SA β-gal activity was determined using the chlorophenol red β-D-galactopyranoside (CPRG) assay. The cells were washed with 1x PBS and lysed using M-PER™ buffer (Thermo Fisher Scientific, Asse, Belgium). Next, 1x CPRG substrate (2 mM chlorophenol red β-D-galactopyranoside in CPRG assay buffer containing 50 mM KPO<sub>4</sub>, 1 mM MgCl<sub>2</sub>, pH 6) (Sigma-Aldrich, Overijse, Belgium) was added and the plate was incubated for 18 h at 37°C without CO<sub>2</sub>. The SA β-gal staining reaction was stopped by addition of 1 M Na<sub>2</sub>CO<sub>3</sub>. The absorbance was measured at 570 nm using a CLARIOstar® Microplate Reader (BMG Labtech, De Meern, The Netherlands). A phenol red standard curve was used for interplate correction. At the start of the assay, cells were stained with Nuclear-ID® Red DNA stain (Enzo Life Sciences, Inc., Brussels, Belgium) and the cell number was determined using the IncuCyte® ZOOM Live-Cell Analysis system and related software (Essen Bioscience, Hertfordshire, United Kingdom).

## 2.5 MUG ASSAY

The cells were seeded in a 96-well plate at 10,000 cells per well. At various time points after irradiation, the SA  $\beta$ -gal activity was determined by conversion of 4-methylumbelliferyl- $\beta$ -D-galactopyranoside (MUG; Invitrogen, Thermo Fisher Scientific, Asse, Belgium) in the fluorescent product 4-methylumbelliferone (4-MU) at pH 6. The cells were washed with 1x PBS and lysed with M-PER™ buffer (Thermo Fisher Scientific, Asse, Belgium) for 5 minutes on ice. Then, reaction buffer (1.7 mM MUG in CPRG assay buffer) was added to each well and the well plate was incubated for 6 h at 37°C without CO<sub>2</sub>. The SA  $\beta$ -gal staining reaction was stopped by addition of 1 M Na<sub>2</sub>CO<sub>3</sub>. The fluorescence was detected with excitation at 360 nm and emission at 465 nm using a CLARIOstar® Microplate Reader (BMG Labtech, De Meern, The Netherlands). A DAPI standard curve was used for interplate correction. At the start of the assay, cells were stained with Nuclear-ID® Red DNA stain (Enzo Life Sciences, Inc., Brussels, Belgium) and the cell number was determined using the IncuCyte® ZOOM Live-Cell Analysis system and related software (Essen Bioscience, Hertfordshire, United Kingdom).

## 2.6 ATORVASTATIN CYTOTOXICITY TEST USING MTT CELL VIABILITY ASSAY

The cells were seeded in a 96-well plate at 10,000 cells per well and treated for 24 h with different concentrations of atorvastatin ranging from 0.1 to 100 nM. 3-(4,5-dimethylthiazol-2-yl)-2,5-diphenyltetrazolium bromide (MTT; Sigma-Aldrich, Overijse, Belgium) was dissolved in 1x PBS at a concentration of 5 mg/ml and filter sterilized. MTT solution was added to all wells (20  $\mu$ l per 100  $\mu$ l medium) and the plate was incubated for 4 h at 37°C. Next, the MTT solution was removed and 175  $\mu$ l of MTT solvent (150  $\mu$ l DMSO and 25  $\mu$ l Sorenson's glycine buffer (0.1 M glycine, 0.1 M NaCl, pH 10.5)) was added to each well. Each well was mixed thoroughly to dissolve all crystals. The absorbance was measured at 570 nm using a CLARIOstar® Microplate Reader (BMG Labtech, De Meern, The Netherlands).

## 2.7 PROTEIN EXTRACTION AND WESTERN BLOT

The cells were seeded in 6-well plates at 300,000 cells per well and cultured in medium containing 100 ng/ml hydrocortisone hemisuccinate from 72 h before irradiation to 7 days after irradiation. Protein extraction was performed using M-PER™ buffer (Thermo Fisher Scientific, Asse, Belgium) after 72 h of treatment with hydrocortisone and on day 7 post irradiation (p.i.). The total protein concentration was determined with the bicinchoninic acid (BCA) assay and compared to the measured absorbance of a bovine gamma globulin (BGG) standard curve. 3 to 5.5  $\mu$ g of total cell lysate was separated on a 4-15% Criterion™ TGX Stain-Free™ precast gel (BioRad, Temse, Belgium) at 300V. Proteins were transferred to a nitrocellulose membrane using the Trans-Blot® Turbo™ Transfer System according to the manufacturer's instructions (BioRad Laboratories, Temse, Belgium). The membrane was blocked with 5% non-fat dried milk powder in TRIS-buffered saline (TBS) with 0.1% Triton-X100 (TBST) for 1 h at room temperature. Next, the membrane was incubated overnight at 4°C with the following primary antibodies: rabbit anti-p16 (SAB4500072, Sigma-Aldrich, Overijse, Belgium), mouse anti-p21 (05-655, Merck Millipore, Overijse, Belgium) and mouse anti-vinculin (sc-73614, Santa Cruz Biotechnology, Inc., Heidelberg, Germany). The secondary antibodies that were used are horseradish peroxidase (HRP) conjugated goat anti-mouse and goat anti-rabbit (Life Technologies, Asse, Belgium). All antibodies were diluted in 5% bovine serum albumin (BSA) in TBST. Enhanced chemiluminescence (ECL) detection was performed using Clarity™ ECL substrate in accordance with the instructions of the manufacturer (BioRad, Temse, Belgium).

## 2.8 NITRIC OXIDE ASSAY

The cells were seeded in a 96-well plate at 13,000 cells per well and cultured in medium with or without 100 ng/ml hydrocortisone hemisuccinate from 72 h before irradiation to 7 days after irradiation. The NO levels were measured by 4-amino-5-methylamino-2',7'-difluorofluorescein diacetate (DAF-FM diacetate; Thermo Fisher Scientific, Asse, Belgium) staining after 72 h of treatment with hydrocortisone and on day 7 p.i. The cells were washed twice with HEPES/HBSS buffer (Hank's Balanced Salt Solution with  $\text{Ca}^{2+}$  and  $\text{Mg}^{2+}$  containing 20 mM HEPES pH 7.2, Thermo Fisher Scientific, Asse, Belgium). Next, the cells were incubated with the DAF-FM staining solution (8.33  $\mu\text{M}$  DAF-FM in HEPES/HBSS buffer) for 30 min in the dark at 37°C. The cells were washed once with HEPES/HBSS buffer and incubated again for 30 min in the dark at 37°C before imaging the cells with a Nikon Eclipse Ti inverted fluorescence microscope equipped with a 20x plan apo dry objective (numerical aperture 0.75). After imaging, S-nitrosocysteine (SNOC; 0.1 M Cys-HCl, 0.1 M  $\text{NaNO}_2$ , 20 nM HCl, 20 nM NaOH, diluted 1:100 in HBSS) was added to each well to a final SNOC concentration of 50  $\mu\text{M}$ . After 15 min of incubation at 37°C in the dark, the plate was imaged again using the same settings as before. SNOC was used as an internal control for this experiment.

## 2.9 IMMUNOCYTOCHEMICAL STAINING

HCAECs were seeded in Lab-tek II chambered slides (Thermo Fisher Scientific, Asse, Belgium) at 50,000 cells per well and cultured in medium with or without 100 ng/ml hydrocortisone hemisuccinate from 72 h before irradiation to 7 days after irradiation. The cells were stained with the senescence detection kit (ab65351; Abcam, Cambridge, UK) using 59.5 mM MUG substrate. After 24 h of incubation, the reaction was stopped by addition of 1 M  $\text{Na}_2\text{CO}_3$ . Next, half of the chambered slides were washed twice with 1x PBS for 5 min and incubated with phalloidin TRITC (Sigma-Aldrich, Overijse, Belgium) and SYBR green (Thermo Fisher Scientific, Asse, Belgium) in 1x PBS for 1 h at room temperature in the dark. The other half of the chambered slides were washed twice with 1x PBS for 5 min after stopping the reaction and incubated with 20% normal goat serum control (Thermo Fisher Scientific, Asse, Belgium) in Tris-HCl NaCl blocking buffer (TNB) (5 g/l TSA blocking reagent, 1x TBST) for 1 h at room temperature. After the blocking, primary mouse anti-p21 (05-655, Merck Millipore, Overijse, Belgium) antibody diluted in TNB was added and the cells were incubated for 2.5 h at room temperature. Next, the cells were washed 3 times with 1x PBS for 5 min. Then, the cells were incubated with secondary Alexa fluor 488 goat anti-mouse antibody (Invitrogen, Thermo Fisher Scientific, Asse, Belgium) diluted in TNB containing phalloidin TRITC (Sigma-Aldrich, Overijse, Belgium) for 1 h at room temperature in the dark. Lastly, all chambered slides were washed two times with 1x PBS for 5 min and mounted with mowiol mounting medium. The cells were imaged using a Nikon Eclipse Ti inverted fluorescence microscope equipped with a 20x plan apo dry objective (numerical aperture 0.75). Cell area and fluorescence intensities were quantified using Fiji by ImageJ.

## 2.10 STATISTICS

All data are given as means  $\pm$  standard error of the mean (SEM). Comparisons between two groups were made using nonparametric Mann-Whitney U test. For multiple groups, statistical significance was determined by Kruskal-Wallis one-way analysis of variance with Dunn's post-hoc test or Two-Way ANOVA with Bonferroni's post-hoc test. P-values < 0.05 were considered as statistically significant.



### 3 RESULTS

#### 3.1 DETECTION OF RADIATION-INDUCED SENESCENCE USING THREE DIFFERENT ASSAYS

Three different assays were performed to detect premature senescence in irradiated (10 Gy) and sham-irradiated (0 Gy) HCAECs. The percentage of senescent cells was determined by standard SA  $\beta$ -gal assay. Additionally, the CPRG and MUG assay were used to quantify the SA  $\beta$ -gal activity after irradiation.

On day 0, the day of irradiation, there is no difference in senescent cells between the irradiated and the sham-irradiated control group (Figure 8).

From day 1 p.i., a difference between both groups can be observed. The results from the standard SA  $\beta$ -gal assay (Figure 8A) and the MUG assay (Figure 8C) show significantly higher SA  $\beta$ -gal activity in the irradiated group compared to the control group. Remarkably, the results from the CPRG assay (Figure 8B) show the opposite with significantly more SA  $\beta$ -gal activity in the control group.

On day 2 p.i., this effect is maintained as illustrated by the results of the CPRG assay. The standard SA  $\beta$ -gal assay also shows significantly more senescent cells in the control group compared to the irradiated group on day 2 p.i. According to the results from the MUG assay, there is no significant difference between both groups at this time point (Figure 8C).

At day 6 p.i., a pronounced effect can be observed with all three assays. The number of senescent cells after irradiation drastically increases on day 6 p.i. and is significantly different from sham-irradiated group. The results from the CPRG and MUG assay also show an increase in SA  $\beta$ -gal activity in the sham-irradiated control group over time.

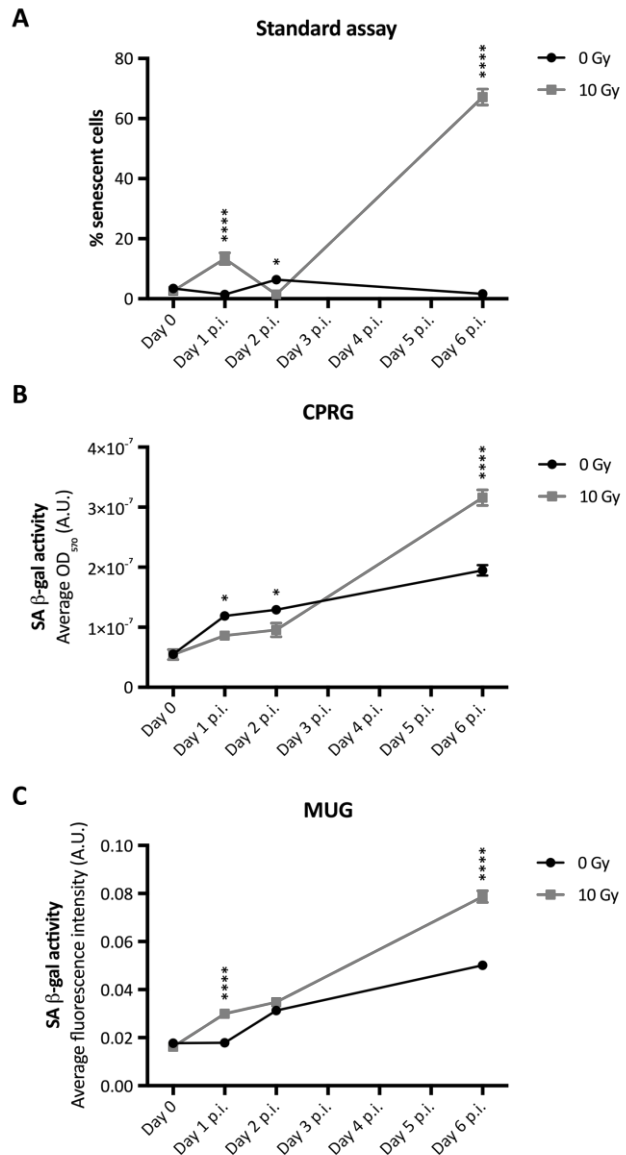


**Figure 8: Senescence-associated  $\beta$ -galactosidase activity (SA  $\beta$ -gal) in irradiated HCAECs.** HCAECs were irradiated with a dose of 10 Gy (0.5 Gy/min) or sham-irradiated. The SA  $\beta$ -gal activity was determined on day 0, 1, 2 and 6 after irradiation using (A) the standard SA  $\beta$ -gal assay ( $n = 9$ ), (B) the CPRG assay ( $n = 12$ ) and (C) the MUG assay ( $n = 12$ ). Data are shown as mean  $\pm$  SEM. \* $P < 0.05$ , \*\*\*\* $P < 0.0001$  compared to sham using Two-Way ANOVA with Bonferroni post-hoc test. A.U.: arbitrary units, OD: optical density, p.i.: post irradiation.

### 3.2 EFFECT OF ATORVASTATIN ON ENDOTHELIAL CELL VIABILITY

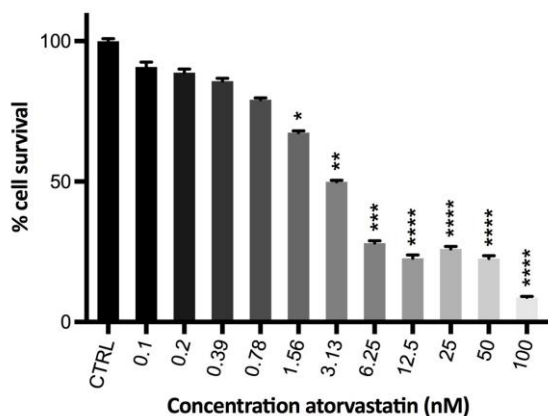


**Figure 9: Effect of atorvastatin on HCAEC viability after 24 h of treatment.** Cell cytotoxicity determined by MTT assay is expressed as percentage of surviving cells and presented as mean  $\pm$  SEM ( $n = 8$ ), \* $P < 0.05$ , \*\* $P < 0.01$ , \*\*\* $P < 0.001$ , \*\*\*\* $P < 0.0001$ , Kruskal-Wallis with Dunn's post-hoc test versus control. CTRL: control.

A cytotoxicity test was performed for atorvastatin because the initially used concentration (100 nM), which was based on literature, induced a considerable amount of cell death. An MTT assay was used to study HCAEC viability in the presence of different concentrations of atorvastatin ranging from 0 to 100 nM. The cytotoxic effects of atorvastatin on HCAECs are illustrated in Figure 9. The results show a decrease in cell survival when the atorvastatin concentration increases. For the lower concentrations, the decrease in cell survival is limited to 20% and not significant. However, concentrations of 1.56 nM and higher induce a considerable amount of cell death. At the highest concentration of 100 nM, only 8.7% of the cells survive. Based on these results, a concentration of 0.4 nM was used for all consecutive experiments.

### 3.3 EFFECT OF DIFFERENT COMPOUNDS ON RADIATION-INDUCED SENEESCENCE IN ENDOTHELIAL CELLS

The high throughput CPRG and MUG assays were used to study the effect of different compounds on the induction of senescence in irradiated (2 Gy) and sham-irradiated (0 Gy) HCAECs. The cells were treated from 72 h before irradiation until 7 days p.i. On the day of irradiation (day 0), after 72 h of treatment with the compounds, the results show a significant increase in senescence in the IGF-1 and hydrocortisone-treated cells. For the other compounds, rosiglitazone, ascorbic acid and atorvastatin, there is no difference in SA  $\beta$ -gal activity compared to the control group (Figure 10A and B).

On day 7 p.i., significant differences in SA  $\beta$ -gal activity can be observed (Figure 10C and D). The increase in senescence by IGF-1 and hydrocortisone treatment in sham-irradiated HCAECs is still present at day 7. Additionally, the results show a significant increase in SA  $\beta$ -gal activity by rosiglitazone treatment on day 7. For ascorbic acid and atorvastatin, no difference can be observed between the sham-irradiated control and sham-irradiated treated cells. Furthermore, both assays show that irradiation with a dose of 2 Gy induces senescence in the untreated control cells. For the treated cells, irradiation induces significantly higher SA  $\beta$ -gal activity in the rosiglitazone-, hydrocortisone- and atorvastatin-treated HCAECs, as shown by the results of the CPRG assay (Figure 10C). According to the results of the MUG assay, irradiation only induces a significant increase in senescence in the atorvastatin-treated cells (Figure 10D). The results of the CPRG as well as the MUG assay show that there is no difference in SA  $\beta$ -gal activity between the sham-irradiated and irradiated HCAECs treated with ascorbic acid or IGF-1. Lastly, the SA  $\beta$ -gal activity is significantly higher in the irradiated cells treated with rosiglitazone, IGF-1 and hydrocortisone compared to the irradiated untreated control cells (Figure 10C and D).

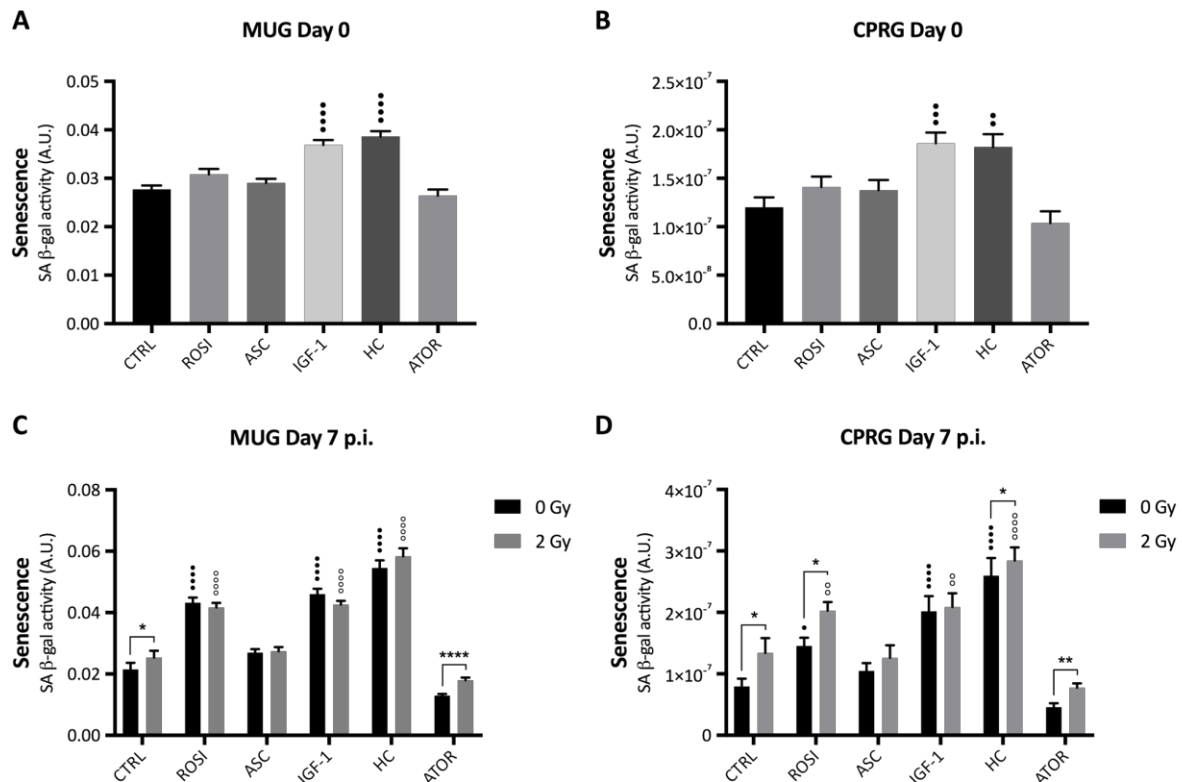


**Figure 10: Senescence-associated  $\beta$ -galactosidase (SA  $\beta$ -gal) activity in irradiated HCAECs treated with different compounds.** HCAECs were treated with rosiglitazone (1  $\mu$ M), ascorbic acid (1 mM), IGF-1 (100 ng/ml), hydrocortisone (100 ng/ml) or atorvastatin (0.4 nM) from 72 h before irradiation until 7 days p.i. HCAECs were irradiated with a dose of 2 Gy (0.5 Gy/min) or sham-irradiated. The SA  $\beta$ -gal activity was determined after 72 h of treatment with the compounds (A and B) and day 7 p.i. (C and D) using the CPRG (A and C) and the MUG assay (B and D). Results were normalized to cell counts. Data are shown as mean  $\pm$  SEM (N = 3, n = 4-16). \*P < 0.05, \*\*P < 0.01, \*\*\*\*P < 0.0001 compared to sham of same treatment, using Mann-Whitney U test. \*P < 0.05, \*\*P < 0.01, \*\*\*P < 0.001, \*\*\*\*P < 0.0001 compared to sham of control, using Kruskal-Wallis test with Dunn's post-hoc test.  $\circ$ P < 0.01,  $\circ\circ\circ$ P < 0.0001 compared to 2 Gy of control, using Kruskal-Wallis test with Dunn's post-hoc test. A.U.: arbitrary units, ASC: ascorbic acid, ATOR: atorvastatin, CTRL: control, HC: hydrocortisone, p.i.: post irradiation, ROSI: rosiglitazone.

### 3.4 EFFECT OF HYDROCORTISONE ON RADIATION-INDUCED EXPRESSION OF P21 AND P16

Based on the previous experiments, hydrocortisone was selected to further study its effect on the radiation-induced senescent phenotype of HCAECs. We opted for hydrocortisone since this compound showed the greatest effect on senescence in endothelial cells. Western blot analysis was performed to determine the effect of hydrocortisone treatment on the expression of p21 and p16 in irradiated (2 Gy) and sham-irradiated (0 Gy) HCAECs. The cells were incubated with hydrocortisone from 72 h before irradiation until 7 days p.i.

Significant differences in p21 protein levels could be observed in a western blot assay. After 72 h of treatment with hydrocortisone (day 0 for radiation exposure), there is a significant decrease in p21 protein levels compared to the control group (Figure 11B). On day 7 p.i., the p21 protein levels are significantly increased in the irradiated control cells compared to the sham-irradiated control cells (Figure 11B). Additionally, irradiation also induced higher p21 protein levels in the hydrocortisone treated cells. However, like on day 0, the p21 protein expression is significantly lower in the hydrocortisone-treated group compared to the control group. This effect is present in the sham-irradiated hydrocortisone-treated cells as well as in the irradiated hydrocortisone-treated cells (Figure 11C).

Western blot analysis of p16 protein expression showed non-specific bands at high exposure times. However, neither of the samples showed specific bands for p16 (Figure S2).

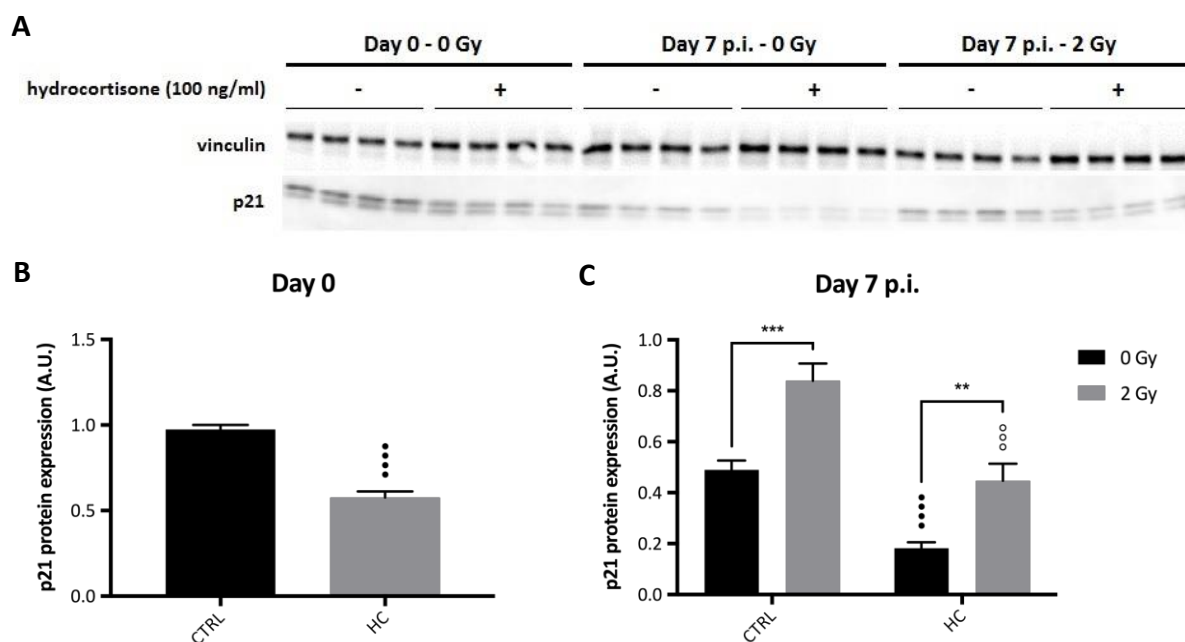


**Figure 11: p21 protein expression in irradiated HCAECs treated with hydrocortisone.** HCAECs were treated with hydrocortisone (100 ng/ml) from 72 h before irradiation until 7 days p.i.. The cells were irradiated with a dose of 2 Gy (0.5 Gy/min) or sham-irradiated. The expression of p21 was determined by western blot (A) after 72 h of treatment with hydrocortisone (day 0 for radiation exposure) (B) and on day 7 p.i. (C). A) Representative blot for p21. Each lane contains 3  $\mu$ g of protein extract. B & C) p21 protein quantification. Data were normalized based on vinculin protein levels. Data are shown as mean  $\pm$  SEM (N = 2, n = 6-8). \*\*P < 0.01, \*\*\*P < 0.001 compared to sham of same treatment, \*\*\*\*P < 0.0001 compared to sham of control,  $\circ\circ\circ$ P < 0.001 compared to 2 Gy of control. The statistical significance was evaluated using Mann-Whitney U test. A.U.: arbitrary units, CTRL: control, HC: hydrocortisone, p.i.: post irradiation.

### 3.5 EFFECT OF RADIATION AND HYDROCORTISONE TREATMENT ON NITRIC OXIDE PRODUCTION BY ENDOTHELIAL CELLS

The intracellular NO bioavailability was assessed in irradiated (2 Gy) and sham-irradiated (0 Gy) HCAECs using the fluorescent NO-sensitive dye DAF-FM. The cells were treated with hydrocortisone (100 ng/ml) from 72 h before irradiation until 7 days p.i. On day 0, the day of irradiation, the hydrocortisone-treated cells have a significantly lower NO bioavailability compared to the control cells (Figure 12A).

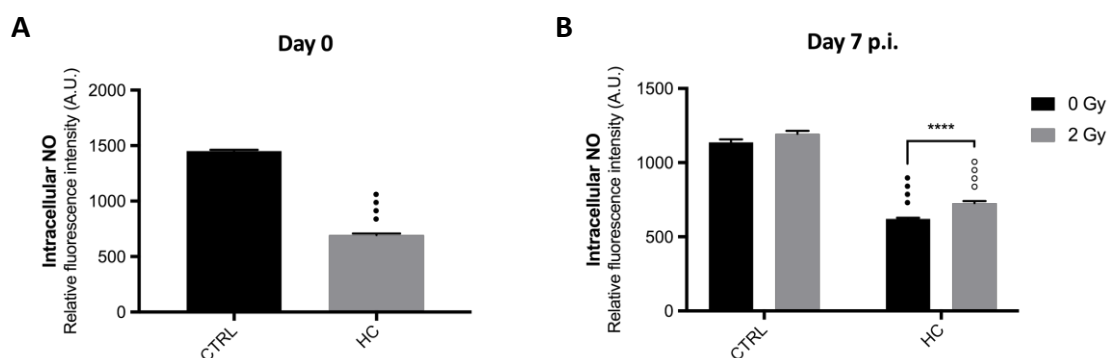


**Figure 12: Intracellular nitric oxide (NO) bioavailability in irradiated HCAECs treated with hydrocortisone.** HCAECs were treated with hydrocortisone (100 ng/ml) from 72 h before irradiation until 7 days p.i.. The cells were irradiated with a dose of 2 Gy (0.5 Gy/min) or sham-irradiated. The NO production capacity was determined after 72 h of treatment with hydrocortisone (day 0 for radiation exposure) (A) and on day 7 p.i. (B) by 4-amino-5-methylamino-2',7'-difluorofluorescein diacetate staining. Data are shown as mean  $\pm$  SEM (N = 1, n = 95). \*\*\*\*P < 0.0001 compared to sham of same treatment using Mann-Whitney U test. \*\*\*\*P < 0.0001 compared to sham of control using Mann-Whitney U test.  $\circ\circ\circ\circ$ P < 0.0001 compared to 2 Gy of control using Mann-Whitney U test. A.U.: arbitrary units, CTRL: control, HC: hydrocortisone, NO: nitric oxide, p.i.: post irradiation.

No difference can be observed between the NO levels of the irradiated and sham-irradiated control cells on day 7 p.i. (Figure 10B). For the hydrocortisone-treated cells, the NO bioavailability is significantly higher in the irradiated cells compared to the sham-irradiated cells. Additionally, the NO levels from the irradiated and sham-irradiated hydrocortisone-treated cells are significantly lower compared to the NO levels of the control cells (Figure 12B).

### 3.6 IMMUNOCYTOCHEMICAL STAINING OF ENDOTHELIAL CELLS

An immunocytochemical staining was performed on sham-irradiated (0 Gy) and irradiated (2 Gy) HCAECs treated with hydrocortisone (Figure 13).

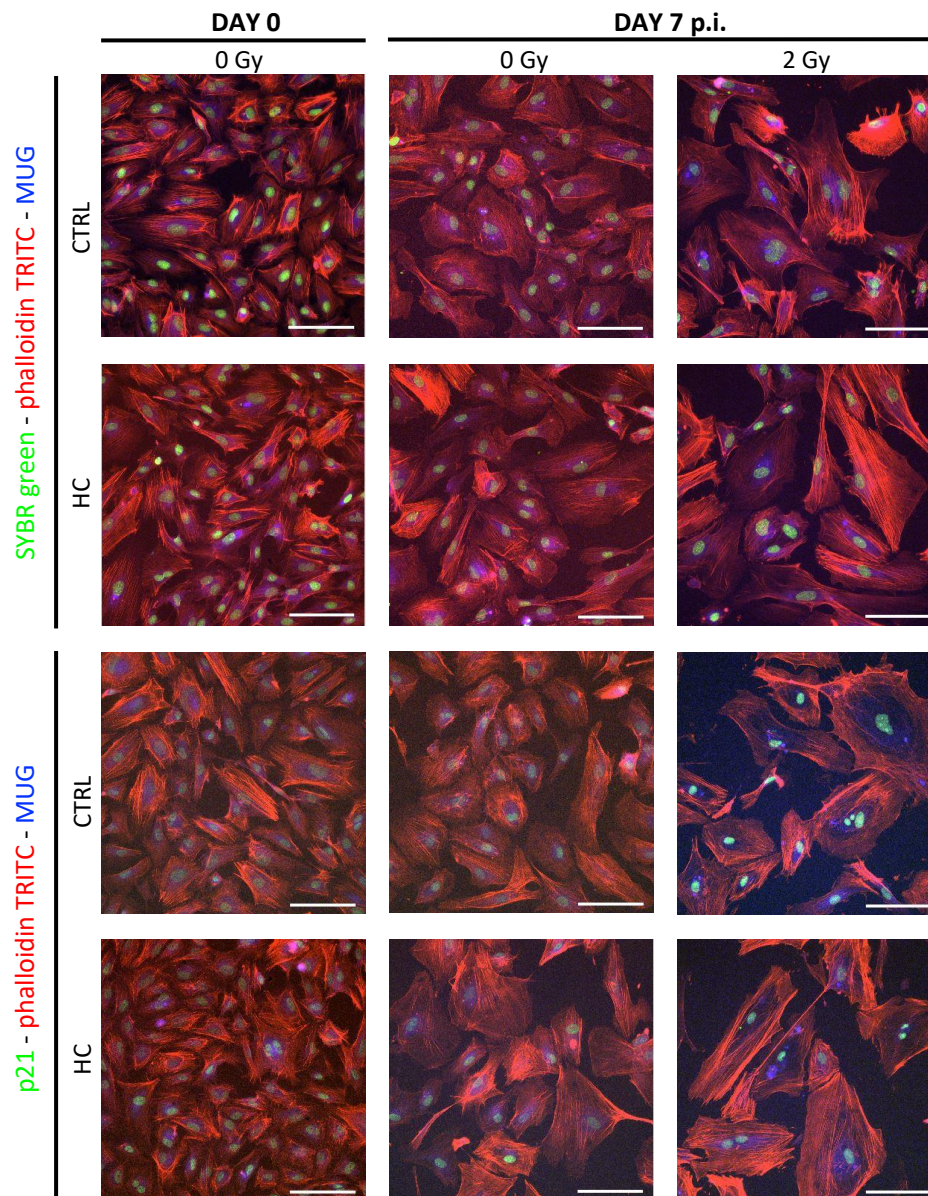


**Figure 13: Immunocytochemical stainings of irradiated HCAECs treated with hydrocortisone.** HCAECs were treated with hydrocortisone (100 ng/ml) from 72 h before irradiation (day 0 of radiation exposure) until 7 days p.i. The cells were irradiated with a dose of 2 Gy (0.5 Gy/min) or sham-irradiated. The cells were stained with SYBR green (nuclei), phalloidin TRITC (actin skeleton) and MUG (senescence-associated  $\beta$ -galactosidase activity) (upper 6 panels) or with phalloidin TRITC, MUG and Alexa fluor 488 goat anti-mouse antibodies against mouse anti-p21 (lower 6 panels). Scale bars represent a distance of 100  $\mu$ m. Image intensity and contrast were adjusted to obtain the highest image quality. CTRL: control, HC: hydrocortisone, MUG: 4-methylumbelliferyl- $\beta$ -D-galactopyranoside.

The cells were stained with SYBR green (nuclei, green), phalloidin TRITC (actin skeleton, red) and MUG (SA  $\beta$ -gal, blue) (Figure 13, upper 6 panels) or with phalloidin TRITC, MUG and Alexa fluor 488 goat anti-mouse antibodies against mouse anti-p21 (green) (Figure 13, lower 6 panels). The images show SA  $\beta$ -gal positive cells that increase in size after irradiation. The SA  $\beta$ -gal positive cells are also positive for p21 expression, which appears to localize in the nuclei (Figure 13).

Cell area as well as MUG and p21 intensities were quantified based on the raw images to reveal quantitative differences between the various conditions (Figure 14). On day 0, there is no significant difference in SA  $\beta$ -gal activity and p21 expression between the hydrocortisone-treated and untreated control cells (Figure 14C and E). Only a significant decrease in cell size could be observed in the hydrocortisone-treated cells compared to the control cells (Figure 14A).

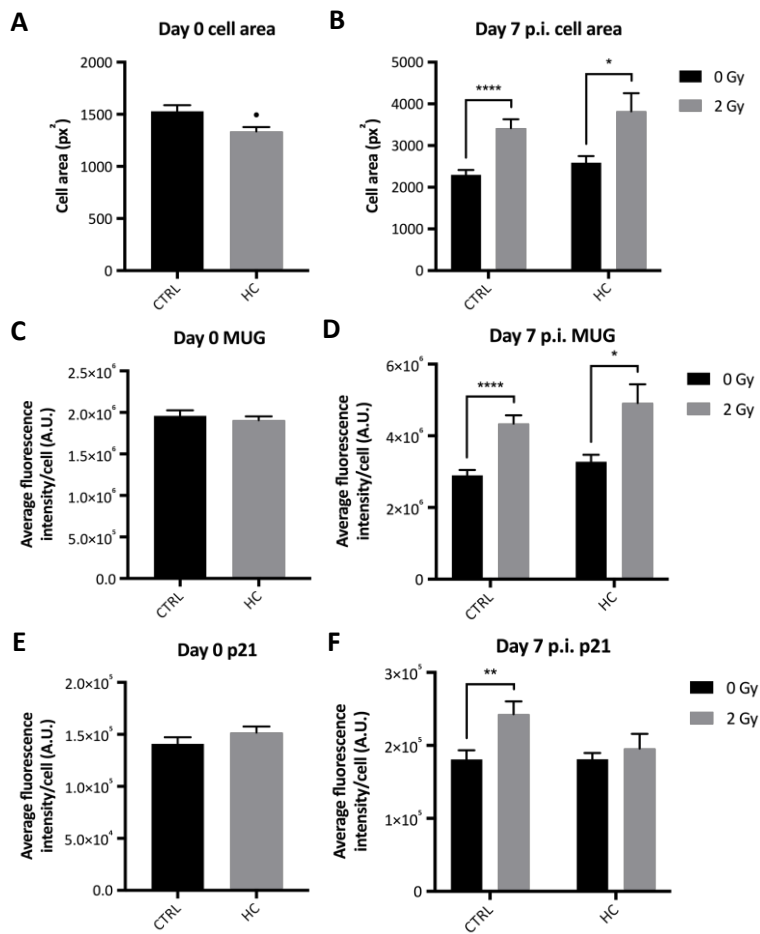


**Figure 14: Ionizing radiation increases cell size, senescence-associated  $\beta$ -galactosidase activity and p21 protein levels in HCAECs.** HCAECs were treated with hydrocortisone (100 ng/ml) from 72 h before irradiation until 7 days p.i. The cells were irradiated with a dose of 2 Gy (0.5 Gy/min) or sham-irradiated. The cells were stained with SYBR green (nuclei), phalloidin TRITC (actin skeleton) and MUG (senescence-associated  $\beta$ -galactosidase activity) or with phalloidin TRITC (actin skeleton), MUG (senescence-associated  $\beta$ -galactosidase activity) and Alexa fluor 488 goat anti-mouse antibodies against mouse anti-p21. A-B) Cell areas based on phalloidin TRITC staining C-D) Senescence-associated  $\beta$ -galactosidase activity based on MUG staining. E-F) p21 protein expression. Areas and intensities were quantified using Fiji by ImageJ based on raw images. Data are shown as mean  $\pm$  SEM (N = 1, n = 12-24). \*P < 0.05, \*\*P < 0.01, \*\*\*\*P < 0.0001 compared to sham of same treatment using Mann-Whitney U test. \*P < 0.05 compared to sham of control using Mann-Whitney U test. A.U.: arbitrary units, CTRL: control, HC: hydrocortisone, p.i.: post irradiation, px: pixels.

On day 7 p.i., cell size is significantly increased in the irradiated HCAECs compared to the sham-irradiated HCAECs (Figure 14B). This applies to the untreated control cells as well as the hydrocortisone-treated cells. No significant difference in cell size could be observed between the control and hydrocortisone-treated cells for both the sham-irradiated and irradiated groups. Furthermore, there is a significant increase in SA  $\beta$ -gal activity between the irradiated and sham-irradiated cells, both for the untreated controls cells as well as the hydrocortisone-treated cells on day 7 p.i. However, there are no significant differences in SA  $\beta$ -gal activity between the control group and hydrocortisone-treated group for both doses (Figure 14D). Lastly, on day 7 p.i., there is a significant increase in p21 protein expression in the irradiated control cells compared to the sham-irradiated control cells. However, in the hydrocortisone-treated cells irradiation does not increase p21 protein expression. Moreover, there is no significant difference in p21 protein expression between the untreated control cells and hydrocortisone-treated cells for both dose groups (Figure 14F).

**Table 2: Summary of all results.** "After treatment" = SA  $\beta$ -gal activity Day 7 0 Gy CTRL vs Day 7 0 Gy treated, "After IR" = SA  $\beta$ -gal activity Day 7 0 Gy treated vs Day 7 2 Gy treated. .CPRG: chlorophenol red  $\beta$ -D-galactopyranoside, IGF-1: insulin-like growth factor-1, IR: ionizing radiation, MUG: 4-methylumbelliferyl- $\beta$ -D-galactopyranoside, NO: nitric oxide, p.i.: post irradiation, SA  $\beta$ -gal: senescence-associated  $\beta$ -galactosidase.

<b>DETECTION OF RADIATION-INDUCED SENESCENCE USING THREE DIFFERENT ASSAYS</b>												
<b>Standard assay</b>			<b>CPRG assay</b>				<b>MUG assay</b>					
↑ number of senescent cells on day 6 p.i.			↑ SA $\beta$ -gal activity on day 6 p.i.				↑ SA $\beta$ -gal activity on day 6 p.i.					
<b>EFFECT OF DIFFERENT COMPOUNDS ON RADIATION-INDUCED SENESCENCE IN ENDOTHELIAL CELLS</b>												
<b>Control</b>		<b>Rosiglitazone</b>		<b>Ascorbic acid</b>		<b>IGF-1</b>		<b>Hydrocortisone</b>		<b>Atorvastatin</b>		
Day 0	Day 7 p.i.	Day 0	Day 7 p.i.	Day 0	Day 7 p.i.	Day 0	Day 7 p.i.	Day 0	Day 7 p.i.	Day 0	Day 7 p.i.	
MUG	/	↑ after IR	No effect	↑ after treatment	No effect	No effect	↑ after treatment	↑ after treatment	↑ after treatment	↑ after treatment	No effect	↑ after IR
CPRG	/	↑ after IR	No effect	↑ after treatment and IR	No effect	No effect	↑ after treatment	↑ after treatment	↑ after treatment	↑ after treatment and IR	No effect	↑ after IR
<b>EFFECT OF HYDROCORTISONE ON RADIATION-INDUCED EXPRESSION OF P21 AND P16</b>												
<b>Control</b>						<b>Hydrocortisone</b>						
Day 0			Day 7 p.i.			Day 0			Day 7 p.i.			
/			↑ p21 levels after IR			↓ p21 levels			↓ p21 levels after 10 days of treatment ↑ p21 levels after IR			
<b>EFFECT OF RADIATION AND HYDROCORTISONE TREATMENT ON NITRIC OXIDE PRODUCTION BY ENDOTHELIAL CELLS</b>												
<b>Control</b>						<b>Hydrocortisone</b>						
Day 0			Day 7 p.i.			Day 0			Day 7 p.i.			
/			No effect after IR			↓ NO production after treatment			↓ NO production after treatment ↑ NO production after IR			
<b>IMMUNOCYTOCHEMICAL STAINING OF ENDOTHELIAL CELLS</b>												
<b>Control</b>						<b>Hydrocortisone</b>						
Day 0			Day 7 p.i.			Day 0			Day 7 p.i.			
/			↑ cell size, SA $\beta$ -gal activity and p21 levels after IR			↓ cell size after treatment No effect on SA $\beta$ -gal activity or p21 levels			↑ cell size and SA $\beta$ -gal activity after IR No effect on p21 levels after IR			



## 4 DISCUSSION

---

The aim of this thesis was to study the effect of various candidate modulators on radiation-induced senescence in endothelial cells. Ionizing radiation can induce senescence in endothelial cells through the induction of DNA damage or ROS production (Rombouts *et al.*, 2014; Yentrapalli *et al.*, 2013a; Yentrapalli *et al.*, 2013b).

To exactly determine the effect of each compound in addition to the effect of ionizing radiation, a comparison should be made based on the sham-irradiated/irradiated ratio, which is not possible with our data. Therefore, comparisons were made between the sham-irradiated and irradiated treated HCAECs and the sham-irradiated and irradiated untreated HCAECs, respectively, as well as the sham-irradiated and irradiated treated HCAECs.

### 4.1 IONIZING RADIATION INDUCES SENESCENCE IN HUMAN CORONARY ARTERY ENDOTHELIAL CELLS

First of all, three different assays were performed to detect radiation-induced senescence in HCAECs. The SA  $\beta$ -gal assay that uses X-gal as substrate, which is considered as the golden standard, and the high throughput alternatives, the CPRG and the MUG assay. On day 0, the day of irradiation, there is no difference in senescence between the irradiated (10 Gy) and sham-irradiated (0 Gy) group, as shown by the results of all three assays. Furthermore, the number of senescent cells is very low on day 0, the day of irradiation. These results are in accordance with our expectations since these cells received the same treatment and were not irradiated. Furthermore, the period of cultivation was short. On day 1 and day 2 p.i., a slight increase in senescence could be observed. In contrast with our expectations, some assays show a significantly higher senescence in the sham-irradiated group compared to the irradiated group. However, the differences between both groups are relatively small. The higher percentage of senescent cells in the sham-irradiated could be due to stress, for example induced by the cell culture conditions. There is evidence that replicative arrest of primary cells may be the result of the stress imposed by cultivation in non-physiologic conditions. For example, disruption of cell-cell contact, inadequate medium-to-cell ratio, lack of appropriate growth factors and plating on plastic are likely to induce stress (Kuilman *et al.*, 2010; Sherr and DePinho, 2000). On day 6 p.i., all three assays show a pronounced increase in senescence. It is known that exposure to ionizing radiation induces senescence in endothelial cells (Baselet *et al.*, 2017; Lowe and Raj, 2014; Rombouts *et al.*, 2014; Yentrapalli *et al.*, 2013a; Yentrapalli *et al.*, 2013b). Thus, as expected, there are significantly more senescent cells in the irradiated group compared to the sham-irradiated group. The results from the CPRG and the MUG assay also show an increase in the number of senescent cells in the sham-irradiated group. This increase could be due to the same reasons mentioned above. Additionally, after a longer period of cultivation the control cells can become senescent since primary cells have a limited replicative lifespan (Hayflick and Moorhead, 1961). Overall, the results show that a radiation dose of 10 Gy induces senescence in endothelial cells, as we expected. The three different assays gave consistent results indicating that the CPRG and MUG assays are good alternatives for the golden standard. For the comparison of the three different assays, a dose of 10 Gy was used as a positive control. For the consecutive experiments, a more clinically relevant dose of 2 Gy was used. Typically, different types of solid tumors are irradiated with doses ranging from 20 to 70 Gy divided in fractions of 1.8 to 2 Gy (Royal College of Radiologists, 2016; Uselmann and Thomadsen, 2015).

### 4.2 ATORVASTATIN INDUCES CELL DEATH IN HUMAN CORONARY ARTERY ENDOTHELIAL CELLS

For atorvastatin, a cytotoxicity test was performed because the initially used concentration (100 nM), which was based on literature and in line with the serum concentration in patients (Gazzerro *et al.*, 2012), induced a considerable amount of cell death. The results from the MTT assay demonstrated a

significant decrease in cell survival at concentrations of 1.56 nM and higher. Based on these results, a concentration of 0.4 nM was used for all subsequent experiments. This concentration is strikingly lower than the concentration of 100 nM used by other research groups. However, other endothelial cells were used in their experiments, which might explain the difference in sensitivity. Furthermore, it is possible that the used atorvastatin molecule is not exactly the same as the one used by other research groups. They received atorvastatin from pharmaceutical companies and therefore, the exact formulation is classified. In our experiments, atorvastatin calcium salt trihydrate was used. It is known that calcium plays an important role in cell death regulation in neurons and other cell types. More specifically, a cellular calcium overload can cause cytotoxicity leading to apoptosis, necrosis or autophagy (Voccoli *et al.*, 2014; Zhivotovsky and Orrenius, 2011). Possibly, the calcium sequestered in the atorvastatin molecule causes a calcium overload in our cell culture leading to cell death. Additionally, there is also evidence that hydrophobic HMG-CoA reductase inhibitors, including atorvastatin, induce apoptosis in rat pulmonary vein endothelial cells. For atorvastatin, they reported that a concentration of 7.9  $\mu$ M reduced the cell viability to 50% (Kaneta *et al.*, 2003). Furthermore, apoptosis was observed in HUVECs treated with hydrophobic statins. Only hydrophobic statins have this effect since hydrophilic statins are unable to penetrate the hydrophobic cell membrane. It was suggested that the inhibition of some geranylgeranylated protein functions by hydrophobic statins leads to apoptotic cell death (Kaneta *et al.*, 2003; Li *et al.*, 2002).

#### 4.3 EFFECT OF DIFFERENT COMPOUNDS ON RADIATION-INDUCED SENESCENCE IN ENDOTHELIAL CELLS

The high throughput CPRG and MUG assays were used to study the effect of different compounds on the induction of senescence in irradiated and sham-irradiated HCAECs treated.

On day 0, after 72 h of treatment with the compounds but no irradiation, the results showed a significant increase in senescence in the IGF-1 and hydrocortisone-treated cells. For rosiglitazone, ascorbic acid and atorvastatin, there was no significant difference compared to the control group, as expected. The increased senescence induced by IGF-1 treatment is in line with our expectations as it is known that prolonged IGF-1 signaling can induce premature senescence through an increase in the expression of p53 and p21 (Handayaningsih *et al.*, 2012; Tran *et al.*, 2014). Hence, this explains the senescence observed in the IGF-1 treated cells. Since hydrocortisone is able to delay the onset of senescence in human fetal lung fibroblasts and can modulate the cell cycle, we hypothesized that hydrocortisone treatment would lead to a decrease in senescent cells (Cristofalo *et al.*, 1985; Phillips *et al.*, 1982). However, we observed an increase in senescence after 72 h of treatment with hydrocortisone. A possible cause for the increased senescence could be enhanced expression of p21 or p27 by hydrocortisone. It has been reported that hydrocortisone treatment increases the expression of p27, which is a cyclin-dependent kinase inhibitor and can induce senescence (Erol *et al.*, 2008; Flores *et al.*, 2014). Other research groups found that glucocorticoids induce the expression of p21 and p27 in various cell types, which can both activate senescence pathways (Reviewed in Pestell *et al.*, 1999). However, the results from the western blot analysis and immunocytochemical stainings do not show an increase in p21 expression by hydrocortisone treatment.

On day 7 p.i., the results from both assays show an increase in senescence in the irradiated control cells compared to the sham-irradiated control cells. Again, this result is in line with our expectations since it was already described that ionizing radiation induces senescence in endothelial cells (Baselet *et al.*, 2017; Lowe and Raj, 2014; Rombouts *et al.*, 2014; Yentrapalli *et al.*, 2013a; Yentrapalli *et al.*, 2013b).

For the rosiglitazone-treated cells, the results indicated that at day 7 p.i. there is a significant increase in senescence for both the irradiated and sham-irradiated cells compared to the untreated control cells. Based on literature, we expected a decrease in senescence because there is evidence that rosiglitazone can decrease ROS accumulation and prevent UV irradiation-induced upregulation of p53

and p21, thereby counteracting a senescent phenotype in fibroblasts (Briganti *et al.*, 2014; Chen *et al.*, 2015). However, the concentrations used by these research groups are higher than the clinically relevant concentration of 1  $\mu$ M used in our experiments (GlaxoSmithKline, 2007). Also, the other research groups performed their experiments with fibroblasts and not endothelial cells. Possibly, the used concentration was too low to prevent the senescence induced by irradiation. Furthermore, UV radiation is non-ionizing and therefore can only induce senescence through accumulation of ROS and indirect DNA damage (Chen *et al.*, 2015; WHO, 2017). Probably, the combination of the low rosiglitazone concentration and the use of ionizing radiation instead of UV radiation are the cause of our unexpected results. Remarkably, the number of senescent cells is also significantly increased in the sham-irradiated HCAECs after 10 days of treatment with rosiglitazone, whereas this was not the case after 72 h of treatment. However, a study by Wakino and colleagues revealed that rosiglitazone has an effect on vascular cell proliferation. More specifically, they found that 24 h of treatment with 10  $\mu$ M rosiglitazone can attenuate p27 degradation in VSMCs (Reviewed in Hsueh *et al.*, 2001; Wakino *et al.*, 2000). If rosiglitazone induces the same effect in endothelial cells, this could explain the increased number of senescent cells in the sham-irradiated group since p27 is a protein involved in the senescence pathway. To conclude, based on these results we can assume that rosiglitazone does not protect against radiation-induced senescence in endothelial cells.

On day 7 p.i., the results from the CPRG and MUG assay indicate that there is no significant difference in senescence between the irradiated and sham-irradiated ascorbic acid-treated cells and the irradiated and sham-irradiated untreated control cells, respectively. Furthermore, there is no significant difference between the irradiated and sham-irradiated ascorbic acid-treated cells. Since irradiation does not increase senescence in the ascorbic acid-treated cells, these results are in line with our hypothesis that ascorbic acid might prevent senescence in endothelial cells. This hypothesis was based on previous research which demonstrated that ascorbic acid can reduce the formation of ROS after irradiation, thereby delaying senescence in endothelial cells and fibroblasts (Haendeler *et al.*, 2004; Kobashigawa *et al.*, 2015). Our results confirm our hypothesis and suggest that ascorbic acid has an effect on radiation-induced senescence in endothelial cells.

The results from day 7 p.i. demonstrate that IGF-1 induces senescence in the sham-irradiated as well as the irradiated cells. These results are in line with the results from day 0 and comply with our expectations. As mentioned before, previous published data demonstrated that prolonged IGF-1 signaling can induce premature senescence through an increase in the expression of p53 and p21 (Handayaningsih *et al.*, 2012; Panganiban and Day, 2013; Tran *et al.*, 2014). Unexpectedly, irradiation does not induce a significant increase in senescence in the IGF-1 treated cells. It is generally known that IGF-1 signaling activates the PI3K/Akt/mTOR pathway (Panganiban and Day, 2013; Rombouts *et al.*, 2014; Tran *et al.*, 2014). Additionally, there are several reports that demonstrate the involvement of the PI3K/Akt/mTOR pathway in the induction of premature senescence in endothelial cells exposed to ionizing radiation (Panganiban and Day, 2013; Rombouts *et al.*, 2014; Yentrapalli *et al.*, 2013b). More specifically, Panganiban and Ray found that a dose of 10 Gy can cause phosphorylation and activation of the IGF1R in human pulmonary artery endothelial cells (HPAECs). The phosphorylation is mediated by X-ray induced ROS and will lead to activation of the PI3K/Akt/mTOR pathway. Furthermore, HPAECs irradiated with a dose of 10 Gy showed a 3.2 fold increase in IGF-1 secretion (Panganiban and Day, 2013). Therefore, we could hypothesize that the treatment with IGF-1 already maximally activates the IGF1R and consequently the PI3K/Akt/mTOR pathway, leading to premature senescence. Possibly, the irradiation with a dose of 2 Gy does not additionally activate the PI3K/Akt/mTOR pathway, which might explain the fact that we do not see an increase in senescence in the IGF-1 treated cells after irradiation. However, further research is necessary to confirm this hypothesis.

For hydrocortisone, the results from day 7 p.i. are consistent with the results from day 0. Hydrocortisone induces a significant increase in senescence in the sham-irradiated cells compared to the untreated control cells. The SA  $\beta$ -gal activity is also significantly higher in the irradiated hydrocortisone-treated group compared to the irradiated untreated group. Like mentioned above, this

increase in senescence may be caused by upregulation of p21 or p27 by hydrocortisone (Erol *et al.*, 2008; Flores *et al.*, 2014; Pestell *et al.*, 1999). Additionally, the results from the CPRG assay show a significant difference between the irradiated and sham-irradiated hydrocortisone-treated cells. This indicates that hydrocortisone is unable to prevent radiation-induced senescence in endothelial cells. Moreover, these data suggest a radiosensitizing effect for hydrocortisone.

On day 7 p.i., there is a slight decrease in senescence in the irradiated and sham-irradiated atorvastatin-treated cells compared to respectively the irradiated and sham-irradiated untreated control cells. However, the decrease is not statistically significant. We hypothesized that atorvastatin may prevent radiation-induced senescence since previous research demonstrated that atorvastatin can prevent ROS formation, decreases p27 expression and increases the expression of eNOS and SIRT1. Furthermore, atorvastatin can prevent senescence in endothelial progenitor cells and HUVECs (Assmus *et al.*, 2003; Ota *et al.*, 2010). Our results show a trend supporting this hypothesis but the difference is not significant. This could be due to the small sample size or the small difference between both groups. This small difference may also be the consequence of the concentration of atorvastatin used in our experiments (0.4 nM). The senescence-preventing effects observed by other research groups were induced by a concentration of 100 nM atorvastatin. Therefore, it could be that a concentration of 0.4 nM, which is 250 times lower, is not sufficient to induce significant differences in senescence. Remarkably, there is a significant difference in senescence between the sham-irradiated and irradiated atorvastatin-treated cells. This suggests that atorvastatin does not have a protective effect against radiation-induced senescence in endothelial cells. However, like mentioned before, the concentration of atorvastatin used in our experiments is probably too low to induce considerable differences. The serum concentrations of atorvastatin in patients range from 2 nM to 100 nM (Gazzero *et al.*, 2012). The concentration used in our experiments is thus even lower than the lowest effective concentration reached in patients. To conclude, further research is necessary to fully elucidate the effect of atorvastatin on radiation-induced senescence in endothelial cells.

Although the results suggest that ionizing radiation and treatment with specific compounds induces senescence in HCAECs, these data should be interpreted with caution. The expression of SA  $\beta$ -gal activity is not a universal marker for senescence despite the fact that it is the most widely used. There are reports that SA  $\beta$ -gal activity can be detected in non-senescent cells at confluence or under serum starvation conditions. Therefore, the detection of SA  $\beta$ -gal activity is ideally combined with other senescence markers like cell cycle arrest, enlarged and flattened morphology, lipofuscin accumulation and senescence-associated  $\alpha$ -fucosidase activity (Georgakopoulou *et al.*, 2013; Lee *et al.*, 2006; Singh and Piekorz, 2013).

The CPRG and MUG assays gave consistent results, which suggests that both assays are suitable to detect SA  $\beta$ -gal activity in endothelial cells.

In the subsequent experiments, the effect of hydrocortisone on the radiation-induced senescent phenotype of HCAECs was further investigated. The effects of the other compounds might be studied in future experiments.

#### **4.4 HYDROCORTISONE TREATMENT REDUCES P21 EXPRESSION IN HUMAN CORONARY ARTERY ENDOTHELIAL CELLS**

Western blot analysis was performed to determine the effect of irradiation and hydrocortisone treatment on p21 and p16 protein expression in HCAECs. P21 and p16 both play an important role in the senescence pathway by inducing a cell cycle arrest (Itahana *et al.*, 2001; Kong *et al.*, 2011; Minamino and Komuro, 2007).

Our results showed that p21 expression was significantly altered by irradiation and hydrocortisone treatment. After 72 h of treatment with hydrocortisone, the p21 protein expression was significantly

lower compared to the control group. On day 7 p.i., the expression was still lower in the hydrocortisone-treated cells compared to the untreated control cells. This result was unexpected because the results of the CPRG and MUG assay suggested an increase in senescence in the hydrocortisone-treated cells on day 0 as well as 7 days after irradiation. It is known that p21 is upregulated in senescent cells (Itahana *et al.*, 2001; Kong *et al.*, 2011), therefore we would expect increased p21 levels in the hydrocortisone-treated cells. Nevertheless, it is possible that the senescence in the hydrocortisone-treated cells is induced by a p21-independent mechanism. For example, there is evidence that hydrocortisone, and glucocorticoids in general, can increase the expression of p27 in diverse cell types (Erol *et al.*, 2008; Pestell *et al.*, 1999). P27 is a cyclin-dependent kinase inhibitor, like p21, that is involved in senescence pathways (Flores *et al.*, 2014). Another possibility is the induction of senescence in the hydrocortisone-treated cells by overexpression of p16, although we were unable to detect p16 expression in the cells. Also, as mentioned before, the expression of SA  $\beta$ -gal activity does not necessarily prove that the cells are senescent since there is no universal marker for senescence (Itahana *et al.*, 2001; Kuilman *et al.*, 2010). Therefore, it is possible that the hydrocortisone-treated cells express SA  $\beta$ -gal activity but are not senescent, which might explain the low p21 levels. Furthermore, there are reports that p21 expression is induced or unaffected by hydrocortisone-treatment in various cell types (Erol *et al.*, 2008; Pestell *et al.*, 1999).

The results also showed that irradiation with a dose of 2 Gy significantly increases p21 expression both in the control and hydrocortisone-treated cells. This result is in line with our expectations because it is known that ionizing radiation-induced DNA damage leads to stabilization and activation of p53. P53 will induce an increase in p21 protein expression, which will cause a cell cycle arrest (Iliakis *et al.*, 2003; Kong *et al.*, 2011). Furthermore, it is known that p21 protein expression is upregulated in senescent cells (Itahana *et al.*, 2001; Kong *et al.*, 2011). The results of the CPRG and MUG assay imply an increase in senescent cells after irradiation with a dose of 2 Gy. Therefore, we can assume that p21 is upregulated in response to ionizing radiation leading to cell cycle arrest and a senescence phenotype in the HCAECs. Irradiation also significantly increased p21 expression in the hydrocortisone-treated cells. This result suggests that hydrocortisone is not able to protect against ionizing radiation-induced upregulation of p21.

The western blot always showed two specific bands for p21. This can be explained by post-translational modifications of p21. For example, Lee and colleagues discovered that p21 is acetylated at lysine 161 and 163 by the acetyltransferase Tip60 in various cell types. Previous studies had already indicated that the acetylase activity of Tip60 increases in response to several stress factors like serum deprivation and DNA damage, including ionizing radiation-induced damage (Lee *et al.*, 2013). Furthermore, there is evidence that p21 can be phosphorylated by various kinases like Pim-1 and Akt at several phosphorylation sites (Rossig *et al.*, 2001; Wang *et al.*, 2002). These post-translational modifications increase the molecular weight of p21, which might explain the presence of the second specific band.

For p16, no specific bands could be detected for all of the samples. We would expect an increase in p16 expression since previous reports indicate that p16 expression is raised in senescent vascular cells (Kong *et al.*, 2011; Minamino and Komuro, 2007). However, the p16/pRb pathway is not always activated in senescence. It is suggested that the p53/p21 pathway is induced by DNA damage and telomere dysfunction, whereas the p16/pRb pathway is activated by oncogenic stimuli and chromatin disruption. In senescent populations, some cells have activated the p53/p21 pathway or the p16/pRb pathway individually or both at the same time, depending on cell type and extent of stress (Kong *et al.*, 2011; Minamino and Komuro, 2007). Furthermore, the dynamics of p16 expression are different compared to p21 expression. There is evidence that p16 expression rises after the senescent phenotype has already been established, while p21 expression increases rapidly in senescent cells (Kong *et al.*, 2011). In human fibroblasts, the p16 levels gradually increase while p21 levels fall several weeks after the cultures reach senescence (Reviewed in Alcorta *et al.*, 1996; Itahana *et al.*, 2001; Stein *et al.*, 1999). Furthermore, Stein and colleagues found that p16 expression only increased after several weeks of senescence and remained elevated for at least two months in human fibroblasts. Therefore,

it is hypothesized that the increase in p16 expression is necessary to maintain the senescent phenotype and growth arrest (Itahana *et al.*, 2001; Stein *et al.*, 1999). Based on this literature, we can assume that 7 days p.i. is too early to detect p16 protein expression in our samples. Lastly, the inability to detect specific bands could also be due to technical problems during the western blot process. For example, the quality of the antibody could have interfered with the result. To rule out this possibility, a positive control should be used in future experiments.

#### 4.5 HYDROCORTISONE TREATMENT REDUCES NITRIC OXIDE PRODUCTION BY HUMAN CORONARY ARTERY ENDOTHELIAL CELLS

NO is generated by eNOS and plays a critical role in vascular homeostasis. The production of NO by endothelial cells is one of the most important anti-atherogenic processes (Fleissner and Thum, 2011).

The intracellular NO bioavailability was assessed in irradiated (2 Gy) and sham-irradiated (0 Gy) hydrocortisone-treated HCAECs using the fluorescent NO-sensitive dye DAF-FM. After 72 h of incubation (on day 0 of radiation exposure), the hydrocortisone-treated cells had significantly lower NO levels compared to the untreated control cells. This result is in line with our expectations since the results of the CPRG and MUG assay indicated significantly higher SA  $\beta$ -gal activity, thus more senescence, in the hydrocortisone-treated cells on day 0 compared to the control cells. It is well-established that senescence decreases the expression and activity of eNOS in endothelial cells. Reduced expression and activity of eNOS will consequently lead to lower NO bioavailability (Bernardini *et al.*, 2005; Matsushita *et al.*, 2001). From the results from day 0 we can conclude that hydrocortisone leads to lower NO bioavailability through senescence-mediated reduced expression and activity of eNOS.

On day 7 p.i., there is no significant difference in NO levels between the irradiated and sham-irradiated control cells. Irradiation induces senescence in HCAECs as indicated by the results of the CPRG and MUG assay, although the difference is small. As mentioned above, senescence decreases eNOS expression and activity leading to lower NO bioavailability. Therefore, we would expect lower NO levels in the irradiated control cells compared to the sham-irradiated control cells. However, despite the induction of senescence by ionizing radiation, there is also evidence that ionizing radiation can influence the expression and posttranslational regulation of eNOS dose-dependently. More specifically, Sonveaux and colleagues found that a dose of 6 Gy significantly increases the expression, phosphorylation and activity of eNOS (Sonveaux *et al.*, 2003). This could be a possible explanation for the higher than expected NO bioavailability in the irradiated control cells. Also on day 7 p.i., the NO levels in the hydrocortisone-treated irradiated and sham-irradiated HCAECs are significantly lower as compared to respectively the irradiated and sham-irradiated control cells. This is in line with our expectations since the results of the CPRG and MUG assay demonstrate that the hydrocortisone-treated cells display significantly higher SA  $\beta$ -gal activity compared to the untreated control cells. However, like with the untreated control cells, the NO bioavailability is higher in the irradiated hydrocortisone-treated cells compared to the sham-irradiated hydrocortisone-treated cells but the difference is very small.

#### 4.6 IRRADIATION INCREASES CELL SIZE, SENESCENCE-ASSOCIATED $\beta$ -GALACTOSIDASE ACTIVITY AND P21 EXPRESSION IN ENDOTHELIAL CELLS

An immunocytochemical staining was performed on sham-irradiated (0 Gy) and irradiated (2 Gy) HCAECs treated with hydrocortisone. We found mostly SA  $\beta$ -gal positive cells that increase in size after irradiation. This is in line with our expectations because irradiation induces senescence in endothelial cells and senescent endothelial cells have an enlarged and flattened cell morphology (Lee *et al.*, 2006; Rombouts *et al.*, 2014; Singh and Piekorz, 2013; Yentrapalli *et al.*, 2013a; Yentrapalli *et al.*, 2013b). Additionally, the results suggest that p21 localizes in the nuclei. This nuclear localization would be in

accordance with the role of p21 as cyclin-dependent kinase inhibitor. It induces a cell cycle arrest which is necessary to repair DNA damage caused by for example ionizing radiation (Cmielova and Rezacova, 2011). Lastly, all SA  $\beta$ -gal positive cells also displayed p21 expression. This was also expected since p21 is an important protein in the senescence pathway and is upregulated in senescent cells (Itahana *et al.*, 2001; Kong *et al.*, 2011).

Cell area as well as MUG and p21 intensities were quantified based on the raw images to reveal quantitative differences between the various conditions. After 72 h of hydrocortisone incubation (on day 0 of radiation exposure), there was a small but significant decrease in cell size in the hydrocortisone-treated cells compared to the control cells. The reason for this reduction in cell size remains unclear and needs further research. Also, there is no significant difference in SA  $\beta$ -gal activity between the control cells and hydrocortisone-treated cells on day 0. This result was not anticipated since the results of the quantitative MUG assay show a significant increase in SA  $\beta$ -gal activity after 72 h of hydrocortisone treatment. Additionally, the observation that 72 h of hydrocortisone treatment does not induce changes in p21 protein expression is in contrast with the results of our western blot analysis. There, we observed a significant decrease in p21 protein expression in the hydrocortisone-treated cells compared to the control cells. These discrepancies might be caused by the staining conditions, which may need further optimization.

On day 7 p.i., there are significant increases in cell size, SA  $\beta$ -gal activity and p21 protein expression in the irradiated control and hydrocortisone-treated cells compared to respectively the sham-irradiated control and hydrocortisone-treated cells. These results are in line with our expectations because it has already been reported that irradiation induces senescence in endothelial cells (Rombouts *et al.*, 2014; Yentrapalli *et al.*, 2013a; Yentrapalli *et al.*, 2013b). The senescent endothelial phenotype is, amongst other things, characterized by an enlarged and flattened cell morphology, increased SA  $\beta$ -gal activity and upregulation of p21 protein expression (Georgakopoulou *et al.*, 2013; Lee *et al.*, 2006; Singh and Piekorz, 2013). However, no significant differences in cell size, SA  $\beta$ -gal activity and p21 protein expression could be observed between the control group and hydrocortisone-treated group for both doses. Based on the results from the CPRG and MUG assay, we would expect increases in cell size and SA  $\beta$ -gal activity in the hydrocortisone-treated cells. In addition, we expected lower p21 protein levels in the hydrocortisone-treated cells compared to the control cells based on the results of the western blot analysis. The explanation for these unexpected results is unclear but since we were unable to reproduce the results from other quantitative assays, it appears that the staining procedure needs further optimization, like mentioned earlier.



## 5 CONCLUSION

---

To date, the endothelial response to ionizing radiation is not fully understood. More specifically, the pathways involved in radiation-induced senescence in endothelial cells remain unclear and need further research. The aim of this thesis was to study the effect of various compounds on radiation-induced senescence in endothelial cells.

First, three different assays were used to detect radiation-induced senescence in endothelial cells. The standard assay, CPRG assay and MUG assay gave consistent results, which indicated that the CPRG and MUG assays are good alternatives for the standard assay. Therefore, these assays were used to determine the effects of the different compounds on radiation-induced senescence in endothelial cells. We found that irradiation with a dose of 2 Gy causes senescence in endothelial cells on day 7 post-irradiation. When studying the effects of the different compounds, we found that 10 days of treatment with 1  $\mu$ M rosiglitazone is not sufficient to prevent radiation-induced senescence in endothelial cells. Furthermore, this prolonged treatment induces senescence, without the involvement of ionizing radiation, probably by increasing the p27 protein levels. Treatment with ascorbic acid did not induce senescence and could attenuate radiation-induced senescence, probably through reduction of ROS formation after irradiation. Moreover, we found that 72 h of IGF-1 treatment led to premature senescence in endothelial cells but irradiation did not have an additional effect on senescence. This might be because both IGF-1 signaling and exposure to ionizing radiation activate the PI3K/Akt/mTOR pathway, leading to premature senescence. Furthermore, we observed that treatment with 0.4 nM atorvastatin was unable to induce significant differences in senescence. Probably, this is due to the low concentration, which is much lower than the serum concentrations in patients ranging from 2 nM to 100 nM. Hydrocortisone led to increased senescence after 72 h of treatment and was unable to prevent radiation-induced senescence on day 7 after irradiation. Possibly, hydrocortisone induces premature senescence by increasing the levels of p21 or p27, which are involved in senescence pathways. Nevertheless, western blot analysis and immunocytochemical stainings did not show an increase in p21 protein levels after treatment with hydrocortisone, although the results were inconsistent. This indicates that hydrocortisone induces premature senescence through a p21-independent mechanism, for example through the p16 or p27 senescence pathways. However, further research is necessary to fully understand the mechanism of hydrocortisone-induced premature senescence. Additionally, we found that hydrocortisone treatment reduces endothelial NO production, which is in line with the increase in senescence observed with the CPRG and MUG assays. Senescence will lead to endothelial dysfunction and therefore less NO production. Lastly, we observed an increase in endothelial cell size induced by irradiation with a dose of 2 Gy, which is consistent with a senescent phenotype.

To conclude, we studied the effects of various compounds on radiation-induced senescence in endothelial cells but further *in vitro* and *in vivo* research is necessary to reveal their potential radioprotective character. Finding a compound that could protect against radiation-induced senescence of endothelial cells will improve our knowledge of the mechanisms involved in this process. Additionally, it might benefit the research on radioprotective drugs.



## 6 REFERENCES

---

- Adams, M.J., Hardenbergh, P.H., Constine, L.S., and Lipshultz, S.E. (2003). Radiation-associated cardiovascular disease. *Crit Rev Oncol Hematol* 45, 55-75.
- Alcorta, D.A., Xiong, Y., Phelps, D., Hannon, G., Beach, D., and Barrett, J.C. (1996). Involvement of the cyclin-dependent kinase inhibitor p16 (INK4a) in replicative senescence of normal human fibroblasts. *Proc Natl Acad Sci U S A* 93, 13742-13747.
- Ashmore, J.P., Krewski, D., Zielinski, J.M., Jiang, H., Semenciw, R., and Band, P.R. (1998). First analysis of mortality and occupational radiation exposure based on the National Dose Registry of Canada. *Am J Epidemiol* 148, 564-574.
- Assmus, B., Urbich, C., Aicher, A., Hofmann, W.K., Haendeler, J., Rossig, L., Spyridopoulos, I., Zeiher, A.M., and Dimmeler, S. (2003). HMG-CoA reductase inhibitors reduce senescence and increase proliferation of endothelial progenitor cells via regulation of cell cycle regulatory genes. *Circ Res* 92, 1049-1055.
- Azizova, T.V., Muirhead, C.R., Druzhinina, M.B., Grigoryeva, E.S., Vlasenko, E.V., Sumina, M.V., O'Hagan, J.A., Zhang, W., Haylock, R.G., and Hunter, N. (2010). Cardiovascular diseases in the cohort of workers first employed at Mayak PA in 1948-1958. *Radiat Res* 174, 155-168.
- Baillargeon, J. (2001). Characteristics of the healthy worker effect. *Occup Med* 16, 359-366.
- Ban, S., Nikaido, O., and Sugahara, T. (1980). Modifications of doubling potential of cultured human diploid cells by ionizing radiation and hydrocortisone. *Exp Gerontol* 15, 539-549.
- Baselet, B., Belmans, N., Coninx, E., Lowe, D., Janssen, A., Michaux, A., Tabury, K., Raj, K., Quintens, R., Benotmane, M.A., et al. (2017). Functional Gene Analysis Reveals Cell Cycle Changes and Inflammation in Endothelial Cells Irradiated with a Single X-ray Dose. *Front Pharmacol* 8, 213.
- Baxter, R.C. (2000). Insulin-like growth factor (IGF)-binding proteins: interactions with IGFs and intrinsic bioactivities. *Am J Physiol Endocrinol Metab* 278, E967-976.
- Bentzon, J.F., Otsuka, F., Virmani, R., and Falk, E. (2014). Mechanisms of plaque formation and rupture. *Circ Res* 114, 1852-1866.
- Bernardini, D., Ballabio, E., Mariotti, M., and Maier, J.A. (2005). Differential expression of EDF-1 and endothelial nitric oxide synthase by proliferating, quiescent and senescent microvascular endothelial cells. *Biochim Biophys Acta* 1745, 265-272.
- Biddle, W. (2012). *A Field Guide To Radiation*. (London: Penguin Books).
- Boivin, J.F., Hutchison, G.B., Lubin, J.H., and Mauch, P. (1992). Coronary artery disease mortality in patients treated for Hodgkin's disease. *Cancer* 69, 1241-1247.
- Brenner, D.J., Doll, R., Goodhead, D.T., Hall, E.J., Land, C.E., Little, J.B., Lubin, J.H., Preston, D.L., Preston, R.J., Puskin, J.S., et al. (2003). Cancer risks attributable to low doses of ionizing radiation: assessing what we really know. *Proc Natl Acad Sci U S A* 100, 13761-13766.
- Brenner, D.J., and Hall, E.J. (2007). Computed tomography--an increasing source of radiation exposure. *N Engl J Med* 357, 2277-2284.
- Briganti, S., Flori, E., Bellei, B., and Picardo, M. (2014). Modulation of PPARgamma provides new insights in a stress induced premature senescence model. *PLoS One* 9, e104045.
- Busse, R., and Fleming, I. (1996). Endothelial dysfunction in atherosclerosis. *J Vasc Res* 33, 181-194.

- Chen, J., Huang, X., Halicka, D., Brodsky, S., Avram, A., Eskander, J., Bloomgarden, N.A., Darzynkiewicz, Z., and Goligorsky, M.S. (2006). Contribution of p16(INK4a) and p21(CIP1) pathways to induction of premature senescence of human endothelial cells: permissive role of p53. *Am J Physiol-Heart C* 290, H1575-H1586.
- Chen, L., Bi, B., Zeng, J., Zhou, Y., Yang, P., Guo, Y., Zhu, J., Yang, Q., Zhu, N., and Liu, T. (2015). Rosiglitazone ameliorates senescence-like phenotypes in a cellular photoaging model. *J Dermatol Sci* 77, 173-181.
- Cmielova, J., and Rezacova, M. (2011). p21Cip1/Waf1 protein and its function based on a subcellular localization [corrected]. *J Cell Biochem* 112, 3502-3506.
- Cristofalo, V.J., Phillips, P.D., and Brooks, K.M. (1985). Cellular senescence: factors modulating cell proliferation in vitro. *Basic Life Sci* 35, 241-253.
- Cristofalo, V.J., and Rosner, B.A. (1979). Modulation of cell proliferation and senescence of WI-38 cells by hydrocortisone. *Fed Proc* 38, 1851-1856.
- Cronstein, B.N., Kimmel, S.C., Levin, R.I., Martiniuk, F., and Weissmann, G. (1992). A mechanism for the antiinflammatory effects of corticosteroids: the glucocorticoid receptor regulates leukocyte adhesion to endothelial cells and expression of endothelial-leukocyte adhesion molecule 1 and intercellular adhesion molecule 1. *Proc Natl Acad Sci U S A* 89, 9991-9995.
- Darby, S.C., Ewertz, M., McGale, P., Bennet, A.M., Blom-Goldman, U., Bronnum, D., Correa, C., Cutter, D., Gagliardi, G., Gigante, B., et al. (2013). Risk of ischemic heart disease in women after radiotherapy for breast cancer. *N Engl J Med* 368, 987-998.
- Davignon, J., and Ganz, P. (2004). Role of endothelial dysfunction in atherosclerosis. *Circulation* 109, III27-32.
- Dimri, G.P., Lee, X., Basile, G., Acosta, M., Scott, G., Roskelley, C., Medrano, E.E., Linskens, M., Rubelj, I., Pereira-Smith, O., et al. (1995). A biomarker that identifies senescent human cells in culture and in aging skin in vivo. *Proc Natl Acad Sci U S A* 92, 9363-9367.
- Erol, E.M., Ugur, M., Öksüz, S., Ersoy, T.F., Esendagli, G., and Güç, D. (2008). The regulation of p21Waf1/Cip1, p27Kip1 and p57Kip2 gene expression in response to hydrocortisone, progesterone and  $\beta$ estradiol in HL-60 myeloid leukemia cells. *Turkish Journal of Cancer* 38, 184-189.
- Erusalimsky, J.D. (2009). Vascular endothelial senescence: from mechanisms to pathophysiology. *J Appl Physiol* (1985) 106, 326-332.
- European Medicines Agency (2016). Avandia (Rosiglitazone). ([http://www.ema.europa.eu/ema/index.jsp?curl=pages/medicines/human/medicines/000268/human\\_med\\_000662.jsp&mid=WC0b01ac058001d124](http://www.ema.europa.eu/ema/index.jsp?curl=pages/medicines/human/medicines/000268/human_med_000662.jsp&mid=WC0b01ac058001d124)).
- Fajardo, L.F., and Stewart, J.R. (1970). Experimental radiation-induced heart disease. I. Light microscopic studies. *Am J Pathol* 59, 299-316.
- Fazel, R., Krumholz, H.M., Wang, Y., Ross, J.S., Chen, J., Ting, H.H., Shah, N.D., Nasir, K., Einstein, A.J., and Nallamothu, B.K. (2009). Exposure to low-dose ionizing radiation from medical imaging procedures. *N Engl J Med* 361, 849-857.
- FDA (2015). FDA Drug Safety Communication: FDA Eliminates the Risk Evaluation and Mitigation Strategy (REMS) for rosiglitazone-containing diabetes medicines. (<http://www.fda.gov/Drugs/DrugSafety/ucm476466.htm>).
- Fleissner, F., and Thum, T. (2011). Critical role of the nitric oxide/reactive oxygen species balance in endothelial progenitor dysfunction. *Antioxid Redox Signal* 15, 933-948.
- Flores, J.M., Martin-Caballero, J., and Garcia-Fernandez, R.A. (2014). p21 and p27 a shared senescence history. *Cell Cycle* 13, 1655-1656.

- Foreman, K.E., and Tang, J. (2003). Molecular mechanisms of replicative senescence in endothelial cells. *Exp Gerontol* 38, 1251-1257.
- Fritz, G., Henninger, C., and Huelsenbeck, J. (2011). Potential use of HMG-CoA reductase inhibitors (statins) as radioprotective agents. *Br Med Bull* 97, 17-26.
- Gazzerro, P., Proto, M.C., Gangemi, G., Malfitano, A.M., Ciaglia, E., Pisanti, S., Santoro, A., Laezza, C., and Bifulco, M. (2012). Pharmacological actions of statins: a critical appraisal in the management of cancer. *Pharmacol Rev* 64, 102-146.
- Georgakopoulou, E.A., Tsimaratou, K., Evangelou, K., Fernandez Marcos, P.J., Zoumpourlis, V., Trougakos, I.P., Kletsas, D., Bartek, J., Serrano, M., and Gorgoulis, V.G. (2013). Specific lipofuscin staining as a novel biomarker to detect replicative and stress-induced senescence. A method applicable in cryo-preserved and archival tissues. *Aging (Albany NY)* 5, 37-50.
- Glanzmann, C., Kaufmann, P., Jenni, R., Hess, O.M., and Huguenin, P. (1998). Cardiac risk after mediastinal irradiation for Hodgkin's disease. *Radiother Oncol* 46, 51-62.
- GlaxoSmithKline (2007). Avandia® (rosiglitazone maleate). ([https://www.accessdata.fda.gov/drugsatfda\\_docs/label/2007/021071s031lbl.pdf](https://www.accessdata.fda.gov/drugsatfda_docs/label/2007/021071s031lbl.pdf)).
- González, A.J. (1994). Biological effects of low doses of ionizing radiation: A fuller picture.
- Haendeler, J., Hoffmann, J., Diehl, J.F., Vasa, M., Spyridopoulos, I., Zeiher, A.M., and Dimmeler, S. (2004). Antioxidants inhibit nuclear export of telomerase reverse transcriptase and delay replicative senescence of endothelial cells. *Circ Res* 94, 768-775.
- Haffner, S.M., Greenberg, A.S., Weston, W.M., Chen, H., Williams, K., and Freed, M.I. (2002). Effect of rosiglitazone treatment on nontraditional markers of cardiovascular disease in patients with type 2 diabetes mellitus. *Circulation* 106, 679-684.
- Hampel, B., Fortschegger, K., Ressler, S., Chang, M.W., Unterluggauer, H., Breitwieser, A., Sommergruber, W., Fitzky, B., Lepperdinger, G., Jansen-Durr, P., et al. (2006). Increased expression of extracellular proteins as a hallmark of human endothelial cell in vitro senescence. *Exp Gerontol* 41, 474-481.
- Handayani, A.E., Takahashi, M., Fukuoka, H., Iguchi, G., Nishizawa, H., Yamamoto, M., Suda, K., and Takahashi, Y. (2012). IGF-I enhances cellular senescence via the reactive oxygen species-p53 pathway. *Biochem Biophys Res Commun* 425, 478-484.
- Hayflick, L., and Moorhead, P.S. (1961). The serial cultivation of human diploid cell strains. *Exp Cell Res* 25, 585-621.
- Herrington, W., Lacey, B., Sherliker, P., Armitage, J., and Lewington, S. (2016). Epidemiology of Atherosclerosis and the Potential to Reduce the Global Burden of Atherothrombotic Disease. *Circ Res* 118, 535-546.
- Home, P.D., Pocock, S.J., Beck-Nielsen, H., Curtis, P.S., Gomis, R., Hanefeld, M., Jones, N.P., Komajda, M., McMurray, J.J., and Team, R.S. (2009). Rosiglitazone evaluated for cardiovascular outcomes in oral agent combination therapy for type 2 diabetes (RECORD): a multicentre, randomised, open-label trial. *Lancet* 373, 2125-2135.
- Hoening, M.J., Botma, A., Aleman, B.M., Baaijens, M.H., Bartelink, H., Klijn, J.G., Taylor, C.W., and van Leeuwen, F.E. (2007). Long-term risk of cardiovascular disease in 10-year survivors of breast cancer. *J Natl Cancer Inst* 99, 365-375.
- Hsueh, W.A., Jackson, S., and Law, R.E. (2001). Control of vascular cell proliferation and migration by PPAR-gamma: a new approach to the macrovascular complications of diabetes. *Diabetes Care* 24, 392-397.

Hull, M.C., Morris, C.G., Pepine, C.J., and Mendenhall, N.P. (2003). Valvular dysfunction and carotid, subclavian, and coronary artery disease in survivors of hodgkin lymphoma treated with radiation therapy. *JAMA* 290, 2831-2837.

ICRP (2007). The 2007 Recommendations of the International Commission on Radiological Protection. ICRP Publication 103. *Ann. ICRP* 37.

Iliakis, G., Wang, Y., Guan, J., and Wang, H. (2003). DNA damage checkpoint control in cells exposed to ionizing radiation. *Oncogene* 22, 5834-5847.

Itahana, K., Dimri, G., and Campisi, J. (2001). Regulation of cellular senescence by p53. *Eur J Biochem* 268, 2784-2791.

Ivanov, V.K., Maksioutov, M.A., Chekin, S., Kruglova, Z.G., Petrov, A.V., and Tsyb, A.F. (2000). Radiation-epidemiological analysis of incidence of non-cancer diseases among the Chernobyl liquidators. *Health Phys* 78, 495-501.

José Luis Silencio Barrita, M.d.S.S.S. (2013). Oxidative Stress and Chronic Degenerative Diseases: A Role for Antioxidants. (InTech).

Kaneta, S., Satoh, K., Kano, S., Kanda, M., and Ichihara, K. (2003). All hydrophobic HMG-CoA reductase inhibitors induce apoptotic death in rat pulmonary vein endothelial cells. *Atherosclerosis* 170, 237-243.

Kim, K.S., Seu, Y.B., Baek, S.H., Kim, M.J., Kim, K.J., Kim, J.H., and Kim, J.R. (2007). Induction of cellular senescence by insulin-like growth factor binding protein-5 through a p53-dependent mechanism. *Mol Biol Cell* 18, 4543-4552.

Kobashigawa, S., Kashino, G., Mori, H., and Watanabe, M. (2015). Relief of delayed oxidative stress by ascorbic acid can suppress radiation-induced cellular senescence in mammalian fibroblast cells. *Mech Ageing Dev* 146-148, 65-71.

Kondo, H., Kasuga, H., and Nourmura, T. (1983). Effects of various steroids on in vitro lifespan and cell growth of human fetal lung fibroblasts (WI-38). *Mechanisms of Ageing and Development* 21, 335-344.

Kong, Y., Cui, H., Ramkumar, C., and Zhang, H. (2011). Regulation of senescence in cancer and aging. *J Aging Res* 2011, 963172.

Kuilman, T., Michaloglou, C., Mooi, W.J., and Peeper, D.S. (2010). The essence of senescence. *Genes Dev* 24, 2463-2479.

Lee, B.Y., Han, J.A., Im, J.S., Morrone, A., Johung, K., Goodwin, E.C., Kleijer, W.J., DiMaio, D., and Hwang, E.S. (2006). Senescence-associated beta-galactosidase is lysosomal beta-galactosidase. *Aging Cell* 5, 187-195.

Lee, M.S., Seo, J., Choi, D.Y., Lee, E.W., Ko, A., Ha, N.C., Yoon, J.B., Lee, H.W., Kim, K.P., and Song, J. (2013). Stabilization of p21 (Cip1/WAF1) following Tip60-dependent acetylation is required for p21-mediated DNA damage response. *Cell Death Differ* 20, 620-629.

Lee, Y.H., Lee, N.H., Bhattarai, G., Yun, J.S., Kim, T.I., Jhee, E.C., and Yi, H.K. (2010). PPARgamma inhibits inflammatory reaction in oxidative stress induced human diploid fibroblast. *Cell Biochem Funct* 28, 490-496.

Li, X., Liu, L., Tupper, J.C., Bannerman, D.D., Winn, R.K., Sebt, S.M., Hamilton, A.D., and Harlan, J.M. (2002). Inhibition of protein geranylgeranylation and RhoA/RhoA kinase pathway induces apoptosis in human endothelial cells. *J Biol Chem* 277, 15309-15316.

Libby, P., Ridker, P.M., and Hansson, G.K. (2011). Progress and challenges in translating the biology of atherosclerosis. *Nature* 473, 317-325.

- Lins, R.L., Matthys, K.E., Verpooten, G.A., Peeters, P.C., Dratwa, M., Stolear, J.C., and Lameire, N.H. (2003). Pharmacokinetics of atorvastatin and its metabolites after single and multiple dosing in hypercholesterolaemic haemodialysis patients. *Nephrol Dial Transplant* *18*, 967-976.
- Little, M.P., Tawn, E.J., Tzoulaki, I., Wakeford, R., Hildebrandt, G., Paris, F., Tapio, S., and Elliott, P. (2008). A systematic review of epidemiological associations between low and moderate doses of ionizing radiation and late cardiovascular effects, and their possible mechanisms. *Radiat Res* *169*, 99-109.
- Lombardi, A., Cantini, G., Piscitelli, E., Gelmini, S., Francalanci, M., Mello, T., Ceni, E., Varano, G., Forti, G., Rotondi, M., et al. (2008). A new mechanism involving ERK contributes to rosiglitazone inhibition of tumor necrosis factor- $\alpha$  and interferon- $\gamma$  inflammatory effects in human endothelial cells. *Arterioscler Thromb Vasc Biol* *28*, 718-724.
- Lowe, D., and Raj, K. (2014). Premature aging induced by radiation exhibits pro-atherosclerotic effects mediated by epigenetic activation of CD44 expression. *Aging Cell* *13*, 900-910.
- Marx, N., Kehrle, B., Kohlhammer, K., Grub, M., Koenig, W., Hombach, V., Libby, P., and Plutzky, J. (2002). PPAR activators as antiinflammatory mediators in human T lymphocytes: implications for atherosclerosis and transplantation-associated arteriosclerosis. *Circ Res* *90*, 703-710.
- Matsushita, H., Chang, E., Glassford, A.J., Cooke, J.P., Chiu, C.P., and Tsao, P.S. (2001). eNOS activity is reduced in senescent human endothelial cells: Preservation by hTERT immortalization. *Circ Res* *89*, 793-798.
- Mehta, K. (2005). Radiation: basic principles. *J Vasc Surg* *42*, 1237-1238.
- Minamino, T., and Komuro, I. (2007). Vascular cell senescence: contribution to atherosclerosis. *Circ Res* *100*, 15-26.
- Minamino, T., Miyauchi, H., Yoshida, T., Ishida, Y., Yoshida, H., and Komuro, I. (2002). Endothelial cell senescence in human atherosclerosis: role of telomere in endothelial dysfunction. *Circulation* *105*, 1541-1544.
- Montecinos, V., Guzman, P., Barra, V., Villagran, M., Munoz-Montesino, C., Sotomayor, K., Escobar, E., Godoy, A., Mardones, L., Sotomayor, P., et al. (2007). Vitamin C is an essential antioxidant that enhances survival of oxidatively stressed human vascular endothelial cells in the presence of a vast molar excess of glutathione. *J Biol Chem* *282*, 15506-15515.
- Murphy, M.P. (2009). How mitochondria produce reactive oxygen species. *Biochem J* *417*, 1-13.
- Naidu, K.A. (2003). Vitamin C in human health and disease is still a mystery? An overview. *Nutr J* *2*, 7.
- NEA OECD (2011). Evolution of ICRP Recommendations 1977, 1990 and 2007. (<https://www.oecd-nea.org/rp/reports/2011/nea6920-ICRP-recommendations.pdf>).
- Nissen, S.E., and Wolski, K. (2007). Effect of rosiglitazone on the risk of myocardial infarction and death from cardiovascular causes. *N Engl J Med* *356*, 2457-2471.
- Nubel, T., Damrot, J., Roos, W.P., Kaina, B., and Fritz, G. (2006). Lovastatin protects human endothelial cells from killing by ionizing radiation without impairing induction and repair of DNA double-strand breaks. *Clin Cancer Res* *12*, 933-939.
- OpenStax Biology (2016). Biological effects of exposure to radiation. ([http://www.alyvea.com/chemistry/effects-radiation.php#CNX\\_Chem\\_21\\_06\\_Damage2](http://www.alyvea.com/chemistry/effects-radiation.php#CNX_Chem_21_06_Damage2)).
- Ostrau, C., Hulsbeck, J., Herzog, M., Schad, A., Torzewski, M., Lackner, K.J., and Fritz, G. (2009). Lovastatin attenuates ionizing radiation-induced normal tissue damage in vivo. *Radiother Oncol* *92*, 492-499.

- Ota, H., Eto, M., Kano, M.R., Kahyo, T., Setou, M., Ogawa, S., Iijima, K., Akishita, M., and Ouchi, Y. (2010). Induction of endothelial nitric oxide synthase, SIRT1, and catalase by statins inhibits endothelial senescence through the Akt pathway. *Arterioscler Thromb Vasc Biol* 30, 2205-2211.
- Panganiban, R.A., and Day, R.M. (2013). Inhibition of IGF-1R prevents ionizing radiation-induced primary endothelial cell senescence. *PLoS One* 8, e78589.
- Pestell, R.G., Albanese, C., Reutens, A.T., Segall, J.E., Lee, R.J., and Arnold, A. (1999). The cyclins and cyclin-dependent kinase inhibitors in hormonal regulation of proliferation and differentiation. *Endocr Rev* 20, 501-534.
- Phillips, P.D., Woolwich, K., and Cristofalo, V.J. (1982). Hydrocortisone stimulation of DNA synthesis in bromodeoxyuridine-selected non-dividing WI-38 cells. *Mech Ageing Dev* 20, 271-277.
- Picciotto, S., Brown, D.M., Chevrier, J., and Eisen, E.A. (2013). Healthy worker survivor bias: implications of truncating follow-up at employment termination. *Occup Environ Med* 70, 736-742.
- Radiological Society of North America (2016). Radiation Dose in X-Ray and CT exams. (<http://www.radiologyinfo.org/en/info.cfm?pg=safety-xray>).
- Reinders, J.G., Heijmen, B.J., Olofsen-van Acht, M.J., van Putten, W.L., and Levendag, P.C. (1999). Ischemic heart disease after mantlefield irradiation for Hodgkin's disease in long-term follow-up. *Radiother Oncol* 51, 35-42.
- Rodríguez, I.R.O., B.B.; Olivar, L.M.; de Lema, A.M. (2015). Chapter 6: Radiation-Induced Heart Disease. In *Cardio-Oncology*, pp. 57-72.
- Roland, J. (2015). Six Statin Drugs and Their Side Effects.
- Rombouts, C., Aerts, A., Quintens, R., Baselet, B., El-Saghire, H., Harms-Ringdahl, M., Haghdoost, S., Janssen, A., Michaux, A., Yentrapalli, R., et al. (2014). Transcriptomic profiling suggests a role for IGFBP5 in premature senescence of endothelial cells after chronic low dose rate irradiation. *Int J Radiat Biol* 90, 560-574.
- Rossig, L., Jadidi, A.S., Urbich, C., Badorff, C., Zeiher, A.M., and Dimmeler, S. (2001). Akt-dependent phosphorylation of p21(Cip1) regulates PCNA binding and proliferation of endothelial cells. *Mol Cell Biol* 21, 5644-5657.
- Royal College of Radiologists (2016). Radiotherapy dose fractionation - second edition. (<https://www.rcr.ac.uk/publication/radiotherapy-dose-fractionation-second-edition>).
- Schultz-Hector, S., and Trott, K.R. (2007). Radiation-induced cardiovascular diseases: is the epidemiologic evidence compatible with the radiobiologic data? *Int J Radiat Oncol Biol Phys* 67, 10-18.
- Shah, D. (2009). Healthy worker effect phenomenon. *Indian J Occup Environ Med* 13, 77-79.
- Sherr, C.J., and DePinho, R.A. (2000). Cellular senescence: Mitotic clock or culture shock? *Cell* 102, 407-410.
- Shimizu, Y., Kodama, K., Nishi, N., Kasagi, F., Suyama, A., Soda, M., Grant, E.J., Sugiyama, H., Sakata, R., Moriwaki, H., et al. (2010). Radiation exposure and circulatory disease risk: Hiroshima and Nagasaki atomic bomb survivor data, 1950-2003. *BMJ* 340, b5349.
- Singh, M., and Piekorz, R.P. (2013). Senescence-associated lysosomal alpha-L-fucosidase (SA-alpha-Fuc): a sensitive and more robust biomarker for cellular senescence beyond SA-beta-Gal. *Cell Cycle* 12, 1996.
- Singh, S., Loke, Y.K., and Furberg, C.D. (2007). Long-term risk of cardiovascular events with rosiglitazone: a meta-analysis. *JAMA* 298, 1189-1195.

- Sonneaux, P., Brouet, A., Havaux, X., Gregoire, V., Dessy, C., Balligand, J.L., and Feron, O. (2003). Irradiation-induced angiogenesis through the up-regulation of the nitric oxide pathway: implications for tumor radiotherapy. *Cancer Res* 63, 1012-1019.
- Spoelhof, B., and Ray, S.D. (2014). Corticosteroids A2 - Wexler, Philip. In *Encyclopedia of Toxicology* (Third Edition) (Oxford: Academic Press), pp. 1038-1042.
- Strandring, W. (2006). Review of the current status and operations at Mayak Production Association. (<http://www.nrpa.no/dav/1fbb52ea04.pdf>).
- Stein, G.H., Drullinger, L.F., Soulard, A., and Dulic, V. (1999). Differential roles for cyclin-dependent kinase inhibitors p21 and p16 in the mechanisms of senescence and differentiation in human fibroblasts. *Mol Cell Biol* 19, 2109-2117.
- Stoneman, V.E., and Bennett, M.R. (2004). Role of apoptosis in atherosclerosis and its therapeutic implications. *Clin Sci (Lond)* 107, 343-354.
- Takahashi, Y. (2012). The regulation of aging and cellular senescence by IGF-1. *Anti-Aging Medicine* 9, 174-179.
- Tran, D., Bergholz, J., Zhang, H., He, H., Wang, Y., Zhang, Y., Li, Q., Kirkland, J.L., and Xiao, Z.X. (2014). Insulin-like growth factor-1 regulates the SIRT1-p53 pathway in cellular senescence. *Aging Cell* 13, 669-678.
- UNSCEAR (2000). Sources and effects of ionizing radiation. ([http://www.unscear.org/unscear/en/publications/2000\\_1.html](http://www.unscear.org/unscear/en/publications/2000_1.html)).
- Uselmann, A.J., and Thomadsen, B.R. (2015). On effective dose for radiotherapy based on doses to nontarget organs and tissues. *Med Phys* 42, 977-982.
- Verheij, M., Dewit, L.G., Boomgaard, M.N., Brinkman, H.J., and van Mourik, J.A. (1994). Ionizing radiation enhances platelet adhesion to the extracellular matrix of human endothelial cells by an increase in the release of von Willebrand factor. *Radiat Res* 137, 202-207.
- Voccoli, V., Tonazzini, I., Signore, G., Caleo, M., and Cecchini, M. (2014). Role of extracellular calcium and mitochondrial oxygen species in psychosine-induced oligodendrocyte cell death. *Cell Death Dis* 5, e1529.
- Vrijheid, M., Cardis, E., Ashmore, P., Auvinen, A., Bae, J.M., Engels, H., Gilbert, E., Gulis, G., Habib, R., Howe, G., et al. (2007). Mortality from diseases other than cancer following low doses of ionizing radiation: results from the 15-Country Study of nuclear industry workers. *Int J Epidemiol* 36, 1126-1135.
- Wakino, S., Kintscher, U., Kim, S., Yin, F., Hsueh, W.A., and Law, R.E. (2000). Peroxisome proliferator-activated receptor gamma ligands inhibit retinoblastoma phosphorylation and G1--> S transition in vascular smooth muscle cells. *J Biol Chem* 275, 22435-22441.
- Wang, Z., Bhattacharya, N., Mixter, P.F., Wei, W., Sedivy, J., and Magnuson, N.S. (2002). Phosphorylation of the cell cycle inhibitor p21Cip1/WAF1 by Pim-1 kinase. *Biochim Biophys Acta* 1593, 45-55.
- WHO (2016a). Cardiovascular diseases (CVDs). (<http://www.who.int/mediacentre/factsheets/fs317/en/>).
- WHO (2016b). Ionizing radiation. ([http://www.who.int/ionizing\\_radiation/about/what\\_is\\_ir/en/](http://www.who.int/ionizing_radiation/about/what_is_ir/en/)).
- WHO (2017). Non-ionizing radiation. ([http://www.who.int/topics/radiation\\_non\\_ionizing/en/](http://www.who.int/topics/radiation_non_ionizing/en/)).
- World Heart Federation (2016). Different Heart Diseases. (<http://www.world-heart-federation.org/cardiovascular-health/heart-disease/different-heart-diseases/>).
- World Heart Federation (2017). Cardiovascular disease risk factors. (<http://www.world-heart-federation.org/cardiovascular-health/cardiovascular-disease-risk-factors/>).

World Nuclear Association (2016). What is radiation? ( <http://www.world-nuclear.org/nuclear-basics/what-is-radiation.aspx>).

Yentrapalli, R., Azimzadeh, O., Barjaktarovic, Z., Sarioglu, H., Wojcik, A., Harms-Ringdahl, M., Atkinson, M.J., Haghdoost, S., and Tapio, S. (2013a). Quantitative proteomic analysis reveals induction of premature senescence in human umbilical vein endothelial cells exposed to chronic low-dose rate gamma radiation. *Proteomics* *13*, 1096-1107.

Yentrapalli, R., Azimzadeh, O., Sriharshan, A., Malinowsky, K., Merl, J., Wojcik, A., Harms-Ringdahl, M., Atkinson, M.J., Becker, K.F., Haghdoost, S., et al. (2013b). The PI3K/Akt/mTOR pathway is implicated in the premature senescence of primary human endothelial cells exposed to chronic radiation. *PLoS One* *8*, e70024.

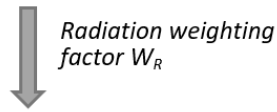
Yusuf, S.W., Sami, S., and Daher, I.N. (2011). Radiation-induced heart disease: a clinical update. *Cardiol Res Pract* *2011*, 317659.

Zhivotovsky, B., and Orrenius, S. (2011). Calcium and cell death mechanisms: a perspective from the cell death community. *Cell Calcium* *50*, 211-221.

Zink, F.E. (1997). X-ray tubes. *Radiographics* *17*, 1259-1268.

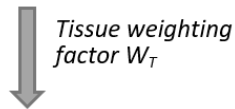
## 7 SUPPLEMENTARY INFORMATION

Absorbed dose (D) in Gray



Equivalent dose ( $H_T$ ) in Sievert

$$H_T = \sum_R W_R \cdot D_{T,R}$$



Effective dose (E) in Sievert

$$E = \sum_T (W_T \cdot H_T)$$

Figure S1: Overview of radiation doses and their units (Based on NEA OECD, 2011).

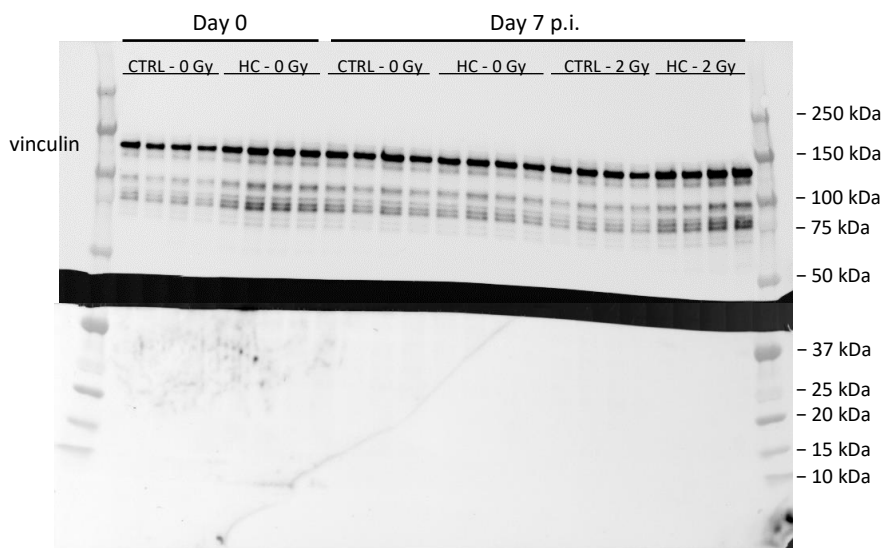


Figure S2: Representative western blot for the analysis of p16 protein levels in irradiated HCAECs treated with hydrocortisone. HCAECs were treated with hydrocortisone (100 ng/ml) from 72 h before irradiation until 7 days p.i. The cells were irradiated with a dose of 2 Gy (0.5 Gy/min) or sham-irradiated. The expression of p16 was determined by western blot after 72 h of treatment with hydrocortisone (day 0) and on day 7 p.i. No specific bands could be detected for p16. CTRL: control, HC: hydrocortisone, p.i.: post irradiation.

*Table S1: Overview of different types of cardiovascular disease (World Heart Federation, 2016).*

<b>Types of cardiovascular diseases</b>	
<b><i>Ischemic heart disease / Coronary artery disease</i></b>	Narrowing of the blood vessels supplying the heart muscle, leading to reduced blood flow to the heart.
<b><i>Angina pectoris</i></b>	Chest pain caused by reduced blood flow to the heart.
<b><i>Myocardial infarction</i></b>	Blood flow to a part of the heart is blocked causing damage to the heart muscle.
<b><i>Cerebrovascular disease / Stroke</i></b>	Narrowing or occlusion of the blood vessels supplying the brain.
<b><i>(Congestive) heart failure</i></b>	Inadequate pumping of blood to the body caused by damage to the heart muscle.



